AMMRC CTR 76-38

EVALUATION OF CONAP CONCEPT FOR ADVANCED ABM NOSETIPS

November 1976

Archie Ossin, Paul Kendall
Martin Marietta Aerospace
Post Office Box 5837
Orlando, Florida 32805

Final Report, Contract Number DAAG46-74-C-0128

Prepared for

ARMY MATERIALS AND MECHANICS RESEARCH CENTER
Watertown, Massachusetts 02172

ACCESSION for

White Section ☑
Buff Section ☐
☐

DISTRIBUTION/AVAILABILITY CODES

Dist. AVAIL. and/or SPECIAL

A

AD

AMMRC CTR 76-38

EVALUATION OF CONAP CONCEPT FOR ADVANCED ABM NOSETIPS

November 1976

Archie Ossin
Paul Kendall

Martin Marietta Aerospace
Orlando Division
P.O. Box 5837
Orlando, Florida 32805

Final Report - Contract DAAG46-74-C-0128 new

D/A Project 1W162113A661
AMCMS Code 62113.11.07000

Prepared for

ARMY MATERIALS AND MECHANICS RESEARCH CENTER
Watertown, Massachusetts 02172

SECURITY CLASSIFICATION OF THIS PAGE (When Data Entered)

REPORT DOCUMENTATION PAGE

READ INSTRUCTIONS BEFORE COMPLETING FORM

1. REPORT NUMBER: AMMRC CTR-76-38	2. GOVT ACCESSION NO.
3. RECIPIENT'S CATALOG NUMBER	
4. TITLE (and Subtitle): Evaluation of CONAP Concept for Advanced ABM Nosetips.	5. TYPE OF REPORT & PERIOD COVERED: Final Report. 29 May 1974 - thru 30 June 1976
	6. PERFORMING ORG. REPORT NUMBER: OR-14228
7. AUTHOR(s): Archie Ossin, Paul Kendall	8. CONTRACT OR GRANT NUMBER(s): DAAG46-74-C-0128 - new
9. PERFORMING ORGANIZATION NAME AND ADDRESS: Martin Marietta Aerospace, P.O. Box 5837, Orlando, Florida 32805	10. PROGRAM ELEMENT, PROJECT, TASK AREA & WORK UNIT NUMBERS: 1W162113A661, AMCMS Code: 62113.11.07000
11. CONTROLLING OFFICE NAME AND ADDRESS: Army Materials and Mechanics Research Center, Watertown, Massachusetts 02172	12. REPORT DATE: November 1976
	13. NUMBER OF PAGES
14. MONITORING AGENCY NAME & ADDRESS (if different from Controlling Office): 91p.	15. SECURITY CLASS. (of this report): Unclassified
	15a. DECLASSIFICATION DOWNGRADING SCHEDULE

16. DISTRIBUTION STATEMENT (of this Report)

Approved for public release; distribution unlimited

17. DISTRIBUTION STATEMENT (of the abstract entered in Block 20, if different from Report)

18. SUPPLEMENTARY NOTES

19. KEY WORDS (Continue on reverse side if necessary and identify by block number)

Missiles	Cooling systems	Porous metals
Anti-missile missiles	Transpiration	
Nose cones	Gas permeability	

20. ABSTRACT (Continue on reverse side if necessary and identify by block number)

This document reports the results of a 25-month research study, entitled "Evaluation of CONAP concept for Advanced ABM Nosetips." This program evaluated the performance of the Controlled Atmosphere Protection (CONAP) concept in active oxidation protection of a hot refractory metal, transpiration cooled nosetip for future application in an Advanced Interceptor Missile system. The specific objectives of this program were to build, process, test, and evaluate three-dimensional porous tungsten, sphere-cone nosetips at the Wright-Patterson 50 MW Plasma Arc Facility. In addition, the program evaluated distributed discrete

DD FORM 1 JAN 73 1473 EDITION OF 1 NOV 65 IS OBSOLETE

403 238

SECURITY CLASSIFICATION OF THIS PAGE (When Data Entered)

LB

PRECEDING PAGE BLANK-NOT FILMED

hole models in the Martin Marietta Ramburner Facility. The porous tungsten nosetips, tested in the 50 MW Plasma Arc Facility were processed porous tungsten made from Sylvania Tungsten-Copper (80 v/o W - 20 v/o Cu), manufactured to SPRINT Specification 11181124. This material selection was based on the results of previous work accomplished under AMMRC Contract DAAG46-73-C-0053 where several porous tungsten materials were characterized for flow properties and internal heat transfer characteristics. The results of these tests showed that the CONAP Concept was viable; however, further development of the porous tungsten material will be required for use in a flight environment. A significant result of the evaluation of the discrete hole concepts was that a departure from the ordinary sphere-cone configuration was advantageous in terms of requiring a minimum flow for survival.

FOREWORD

This Final Report (OR 14,228) was prepared by Martin Marietta Aerospace Orlando Division for the Army Materials and Mechanics Research Center, Watertown, Massachusetts, under Contract DAAG46-74-C-0128, entitled "Evaluation of CONAP concept for Advanced ABM Nosetips." This work is part of the AMMRC program on Development of Hardened ABM Materials, Mr. John F. Dignam, program manager. The AMMRC technical supervisor is Mr. Lewis Aronin.

The work reported herein was performed from 29 May 1974 through 30 June 1976. Mr. Archie Ossin was the task leader and Mr. William A. Bauman was program manager.

CONTENTS

ILLUSTRATIONS

TABLES

SUMMARY

This document reports the results of a 25-month research study, entitled "Evaluation of CONAP concept for Advanced ABM Nosetips." This program evaluated the performance of the Controlled Atmosphere Protection (CONAP) concept in active oxidation protection of a hot refractory metal, transpiration cooled nosetip for future application in an advanced interceptor missile system. The specific objectives of this program were to build, process, test, and evaluate three-dimensional porous tungsten, sphere cone nosetips at the Wright-Patterson 50 MW Plasma Arc Facility. In addition, the program evaluated distibuted discrete hole models in the Martin Marietta Ramburner Facility. The porous tungsten nosetips tested in the 50 MW Plasma Arc Facility were processed from Sylvania Tungsten-Copper (80 v/o - 20 v/o Cu), manufactured to SPRINT Specification 11181124 (Appendix III). This material selection was based on the results of previous work accomplished under AMMRC Contract DAAG46-73-0053 where several porous tungsten materials were characterized for flow properties and internal heat transfer characteristics.

The testing conducted in the 50 MW facility was intended to compare and evaluate the performance of porous nosetip designs in a three-dimensional environment. The results of this test (summarized in Table I and shown in Figures 1 and 2) show that: 1) two porous tungsten models (models No. 4 and 5) performed well for the total test time of 4 seconds, 2) one model performed well for 1.2 seconds and subsequently broke at the neck, 3) one model failed at 0.5 second, and 4) the remaining two models did not receive sufficient coolant because of expulsion system venting. Of the five porous tungsten models tested, three porous models cracked longitudinally along the sidewall, and one broke at the neck during the tests. Only one of the models had no apparent cracking. Based upon this performance, it was concluded that, in principle, the CONAP porous tungsten matrix concept using a reactive gas operates successfully. The matrix material, however, will require considerable development to qualify as a flight system nosetip candidate.

The significant result of the evaluation of the discrete hole concepts was that a departure from the ordinary sphere-cone configuration was advantageous in terms of requiring a minimum flow for survival. Two concepts in particular required less coolant than others considered: 1) the 30-degree ogive configuration with sideslots and 2) the sphere-cone-cone configuration with sideslots (shown in Figure 3).

Based upon the results of this program it was concluded that future work in the development of the CONAP concept should concentrate on the following:

1 Development of porous tungsten material.

2 Assessment of discrete hole concepts at angle-of-attack.

3 Testing of the discrete hole concept in a plasma arc facility.

4 Assuming that viability of both concepts is demonstrated, combined ablation-erosion testing followed by full-scale ground tests in a rocket exhaust facility should be performed.

TABLE I

Test Results at Wright-Patterson 50 MW Plasma Arc

	Model No.	Description	Results	Model Condition
20 blind holes equally spaced at 45 degrees, each hole 0.02 in dia x.025 in depth; 45°; 5μ vapor deposit	7	Porous tungsten 5μ tungsten on sidewall Blind holes	• Model split longitudinally at 0.5 seconds	• Not recovered
5μ vapor deposit	8	Porous tungsten 5μ tungsten on 1 sidewall	• Low pressure flow to this model because strut no. 1 model vented • Ablated to expose internal hole	• Longitudinal crack on sidewall
3μ vapor deposit	4	Porous tungsten 3μ tungsten on sidewall	• Survived for total test time of 4 seconds • Small amount of ablation at stagnation point	• No longitudinal cracking • No known subsidiary cracks
20 blind holes equally spaced at 45 degrees each hole 0.02 inch dia x 0.025 inch depth; 45°; 3μ vapor deposit	5	Porous tungsten 3μ tungsten on sidewall Blind holes	• Survived for total test time of 4 seconds • Gas vented through crack near end of test and starved stagnation point and blind hole area	• Longitudinal crack • Subsidiary cracks
1μ vapor deposit	3	Porous tungsten 1μ tungsten on sidewall	• Broke at neck at 1.2s test time • Data showed that nose tip was working well	• Nose tip in good shape
60°; 30°; 0.025R; A; 30°; 60°; A; Drill 13 holes 0.020 dia	9	Tungsten-Cu Discrete holes	• Supply pressure roughly equal to stagnation pressure of facility (20 atm) • Ablated at stagnation point and exposed internal hole	• Ablation ceased when internal hole was exposed

Test conducted at:
H_{STAG} = 3800 Btu/lb q_{STAG} = 4000 Btu/ft^2-s
P_{STAG} = 20 atm Test time = 4 seconds

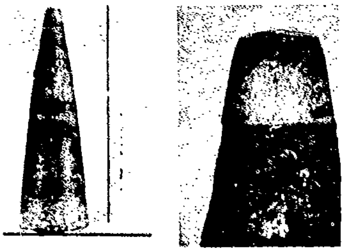

Figure 1. Post Test of Porous Tungsten Nosetip No. 4 Tested for 4 Seconds

Figure 2. Post Test of Porous Tungsten Nosetip No. 5 Tested for 4 Seconds

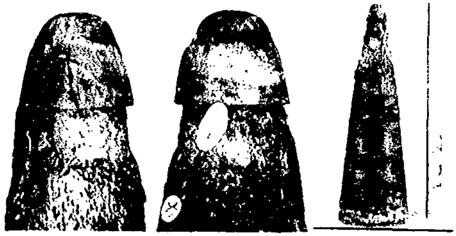

DESCRIPTION	CONFIGURATION	
CONFIGURATION 3 SPHERE-CONE-CONE WITH 1/8-INCH CENTERLINE HOLE AND SIDE-SLOTS		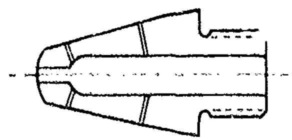
CONFIGURATION 5 30-DEGREE OGIVE WITH 1/8-INCH CENTERLINE HOLE AND SIDESLOTS		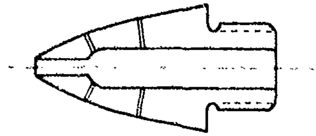

Figure 3. CONAP Discrete Hole Configuration Tested in Ramburner

1.0 INTRODUCTION

1.1 Background

High performance interceptors require the development of a low recession, shape stable, erosion resistant nosetip. The development of nosetips for advanced systems is currently persuing both active and passive concepts. The use of orthogonal-weave carbon/carbon nosetips with refractory metal subtips for erosive environments represents one approach. Actively cooled systems based on both liquid and gas coolants are an alternative approach. This study is concerned with development of an active gas-cooled nosetip.

Use of a coolant transpired through a metal matrix wall or through a distributed discrete hole matrix wall as a heat protection surface for the nosetip of a hypersonic vehicle is not new. It has been receiving considerable attention in recent years as a means of achieving a shape-stable nosetip for high ballistic factor reentry vehicles (References 2, 3, 4, and 5). Ground and flight tests have been conducted on systems with water as the coolant and stainless steel as the matrix, with the coolant introduced to the wall surface through either discrete holes or by distributed porosity. The basic principles are well proven and, although there are uncertainties in the downstream cooling effectivity of the fluid film layer and a required safety factor, transpiration cooling has been used in practice (Reference 6) to provide zero-recession nosetips under the most severe ICBM reentry conditions.

Although water has a relatively high efficiency as a coolant and has a good storage density, the work of References 1, 5 and 7 shows that if water is replaced as a coolant by a reactive gas used with a high surface temperature porous matrix, or with a warm dilutant gas expelled from a discrete hole refractory matrix, numerous system benefits could theoretically be realized. These include lower coolant weights and lower expulsion system weights. A material that can operate at a high surface temperature is an ideal matrix material since high surface temperatures greatly reduce the net incoming heat flux. Also, with a material that can operate at a high temperature, local hot spots are not catastrophic. A refractory metal such as tungsten, would be an excellent material for this application except that at high surface temperatures the tungsten must be protected from the oxidizing effects of the boundary layer oxygen.

The Controlled Atmosphere Protection (CONAP) concept combines a reactive coolant, ammonia, or a dilutive coolant with the high temperature tungsten matrix. This concept depends upon the ability of the injected coolant to either deplete or dilute the flow of oxygen reaching the refractory hot wall. A series of tests was conducted to demonstrate experimentally the feasibility of this concept (References 7 and 8). In the first series, (Reference 7) ammonia coolant was used in conjunction with a porous tungsten matrix.

The results of these tests, conducted at the AVCO 10 MW Plasma Arc Facility, showed that at a heat flux of 3500 BTU/ft^2-s and an enthalpy of 4000 BTU/lb no measurable recession occurred in a 5-second test where ammonia was used to deplete oxygen at the surface of a porous tungsten matrix.

In the second series of tests (Reference 8) a dilutant coolant was used with a discrete hole matrix. The results of these tests, conducted in the Martin Marietta Ramburner Facility, showed the survival of a surrogate material (aluminum) with no recession.

It has been anticipated that in the CONAP concept using porous tungsten materials, the porous materials matrix development and the internal coolant flow distribution would be the key problems to be addressed, whereas an angle-of attack environment would be of minimal effect on this type of nosetip. In the CONAP concept using a discrete hole matrix, the external configuration and angle-of-attack would be the key problems, whereas the development of a suitable refractory metal would not be as critical since high strength refractory metals were previously developed in a related AMMRC contract (Reference 9).

The initial study in the development of the CONAP concept was conducted under contract to the Army Materials and Mechanics Research Center, Contract DAAG46-73-C-0053. This study concentrated on quantifying the pressure and thermal response of the gas passing through the porous matrix and the mechanics of controlling the flow in the porous matrix. The purpose of the initial study was to evaluate available porous refractory materials and their applicability as nosetip or air vane leading edge materials in a flight environment. Flow characteristics of the materials and the operating efficiency of the concept were evaluated by laboratory testing. These tests consisted of obtaining flow characteristic data (permeability and inertial resistance coefficient) for a variety of porous tungsten and discrete hole tungsten matrices. The heat transferred from a hot tungsten matrix to the ammonia gas passing through the matrix was also measured. The materials and concepts that were evaluated and the tests performed are shown in Table 1-I. A wide range of porous tungsten materials, ranging from 50 percent (by volume) tungsten to 80 percent tungsten were evaluated, and complete correlations of the data were obtained. Based on these data, several conclusions were made. At the coolant mass flow rates expected 5 lb/ft^2-s) for a typical advanced interceptor environment, the internal heat transfer coefficient is on the order of 1000 BTU/ft^3-s°R. The impact of this result on the system weight is discussed in Reference 1; it was found that the CONAP concept system weights are roughly 50 percent lighter than the water system weights. The flow characteristics data show that the porous tungsten matrices, augmented with blind holes, can increase the coolant mass flow rate in a local area without starving other surface areas for coolant. The combination of flow characteristics data and heat transfer coefficient data shows that the process of surface vapor deposition decreases coolant mass flow in a local area without affecting the heat transfer coefficient. These modifications to a porous tungsten material can be used to tailor the coolant mass flow distribution through the porous matrix to better meet the mass flow requirement distribution of a nosetip or air vane leading edge. The blind hole technique can be used in the sonic point region of a nosetip or stagnation line region of an air vane leading edge to increase the local mass flow. The vapor deposition technique can be used on the sidewall on both parts to decrease the local mass flow. These experimental results applied to a flight environment made it possible to define the best of the available porous tungsten materials. As discussed in Reference 1, the Wah Chang and Sylvania porous tungsten (80 percent by volume) materials were selected as the best of the available porous tungsten materials. This selection was based upon those materials whose design, through the flow modifications discussed, resulted in the minimum flow rate variation between actual and ideal flow.

TABLE 1-I

Material and Test Summary (Reference 1)

Flow Direction	Materials and Concepts Evaluated
⇨	Porous tungsten
⇨ ⇦	Porous tungsten modified with blind holes to increase flow
⇨	Porous tungsten modified with vapor deposition to decrease flow
⇨	Discrete hole tungsten - copper
	Test Conducted
	• Internal heat transfer coefficient • Flow characteristics tests (permeability and inertial resistance coefficient)

In the initial CON^{AP} study, a one-dimensional experimental and analytical approach was used to evaluate and select the most nearly optimum materials and concepts. The three-dimensional effects were evaluated analytically; however, the experimental evaluation of nosetip shapes can best be accomplished in a high pressure plasma arc facility which is the basis of the current experimental program.

The CONAP concept using a discrete hole matrix represents a logical extension of the initial effort and offers the advantage of having a more structurally sound material.

1.2 Study Approach and Objectives

The study discussed in the present report assessed the performance of three-dimensional nosetips in both the Wright-Patterson 50 MW Plasma Arc Facility and the Martin Marietta Ramburner Facility.

The goals of this test program were to:

1. Compare and evaluate the performance of porous nosetip designs in a three-dimensional environment in the Wright-Patterson 50 MW Plasma Arc Facility

2. Compare the performance of several discrete hole configuration concepts in the Martin Marietta Ramburner Facility.

2.0 PLASMA ARC TEST PROGRAM

2.1 Nosetip Design and Tungsten Materials Selection

2.1.1 Nosetip Description

Nosetips evaluated in this program consisted of six porous tungsten nosetips and one discrete holed tungsten copper tip. Five of the porous tungsten tips were modified wich blind holes and vapor-deposited tungsten on the sidewalls to permit tailoring of the gas flow. The basic nosetip design is shown in Figure ?-1. The interconnected porosity tungsten matrix, required for coolant gas flow in the transpiration cooling process, was achieved through copper extraction of the tungsten-copper stock, purchased to SPRINT Specification 11181124 (Appendix III). All of the tips were machined from tungsten copper stock to the configuration of Figure 2-1, prior to further processing to achieve the final configurations. In the case of the porous tungsten nosetips, this additional processing included copper extraction, which will be described later in this section, the application of vapor deposited tungsten material on the nosetip sidewall and the drilling of blind holes in the nosetip hemispherical section at the 45 degree surface angle point. The nosetip processing sequence, in the order of execution, was as follows: The nosetips were first machined to the configuration of Figure 2-1. The copper phase in the material significantly contibutes to the ease of machining of this material. Blind holes were then drilled into the appropriate nosetips. Porous tungsten parts were then obtained through the copper extraction process. Finally, tungsten vapor was deposited upon the sidewall of the appropriate nosetips. The purpose of the blind holes, placed at the nosetip sonic point, and the tungsten material vapor deposited upon the nosetip sidewall, was to locally increase and decrease coolant flow rate, respectively, in order to tailor the distribution of coolant flow to the requirements imposed by the aerodynamic heating distribution about the nosetip, as discussed in reference 1. In the case of the discrete hole tungsten nosetip, the additional processing beyond the machining of the tungsten-copper rod to the configuration of Figure 2-1, included only the drilling of 13 discrete holes from the surface of the nosetip through the material to the inside plenum.

Detailed descriptions of the final nosetip configurations are shown in Table 2-I. Nosetips 1 and 2 were both porous tungsten nosetips with no additional modifications to tailor the coolant flow. Porous tungsten nosetips 3, 4 and 8 were all modified with tungsten vapor deposited on the sidewall, as shown in Table 2-I. Porous tungsten nosetips 5 and 7 were modified with 20 blind holes, equally spaced, at the sonic point located at the nosetip location where the local surface angle is 45 degrees, and with tungsten vapor desposited upon the sidewall. Nosetips 6 and 9 were made of tungsten-copper, with discrete holes drilled into the tip region. During the drilling process of nosetip 6, two tungsten-carbide drills being used broke and were lodged inside the discrete holes. This nosetip was not processed any further, and was not used in the remainder of the program. Nosetip 9 contained 13 discrete holes, each measuring 0.030 inch diameter. One hole was placed at the stagnation point; six holes, equally spaced, were placed at the 30-degree location, and six holes, equally spaced, were placed at the 60-degree location.

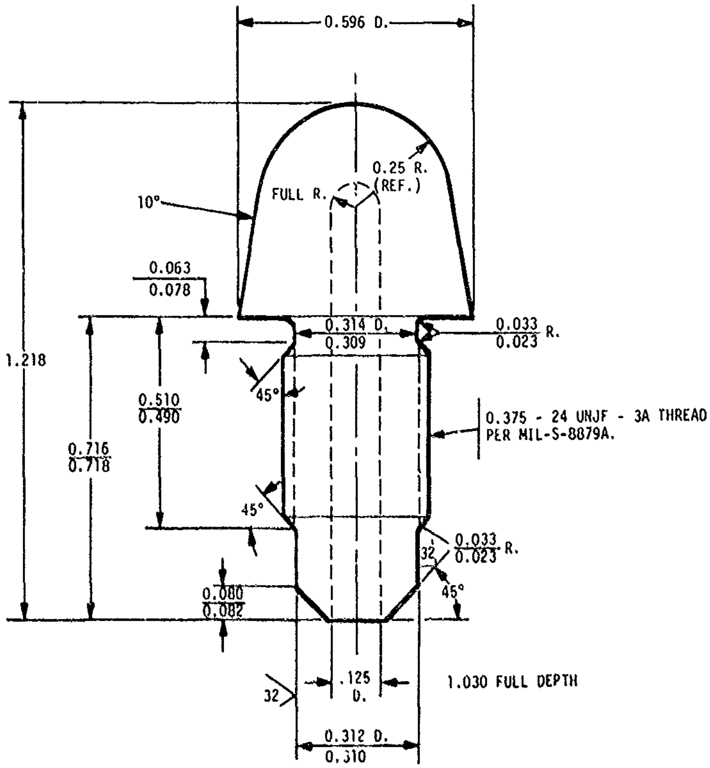

Figure 2-1. Nosetip Model

TABLE 2-I

Description of Fabricated Nosetips

Nosetip Model Number	Description	Model Configuration
1.	Porous tungsten	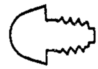
2	Porous tungsten	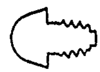
3	Porous tungsten with 1μ of tungsten vapor deposited upon the sidewall	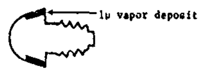
4	Porous tungsten with 3μ of tungsten vapor deposited upon the sidewall	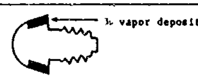
5	Porous tungsten with 3μ of tungsten vapor deposited upon the sidewall and with 20 blind holes, equally spaced, at 45 degrees, each hole measures .020 inch dia x .025 inch deep	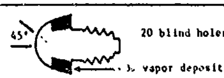
6	Tungsten-copper, discrete holes (damaged during drilling process)	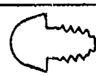
7	Porous tungsten with 5μ of tungsten vapor deposited upon the sidewall and with 20 blind holes, equally spaced, at 45 degrees, each hole measures .020 inch dia x .025 inch deep	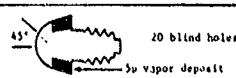
8	Porous tungsten with 5μ of tungsten vapor deposited upon the sidewall	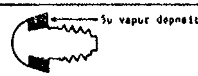
9	Tungsten-copper with 13 discrete holes measuring .030 inch dia. One hole placed at stagnation point, six holes, equally spaced, at 30 degrees and at 60 degrees.	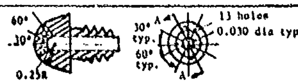

2.1.2 Porous Tungsten Materials

The selection of porous tungsten nosetip materials to be tested in this program at the Wright-Patterson Plasma Arc Facility was based on the results of the tests and analyses conducted under AMMRC Contract DAAG46-73-C-0053 (Reference 1). It was found in that study that porous tungsten matrices processed from the 80/20 tungsten-copper (80 v/o W - 20 v/o Cu) were superior to the other materials in minimizing the coolant flow rate variation between actual and ideal flow.

The 80 v/o W - 20 v/o Cu material used for the nosetip test specimen in this test series, was manufactured by Sylvania. It is an interconnected pore tungsten matrix, infiltrated with copper, and meets SPRINT Specification 11181124 (Appendix III). Prior to the acceptance of this material, a metallurgical examination was made of the microstructure of the specimens of tungsten-copper provided by Sylvania. The paragraph in the SPRINT Specification dealing with the microstructure limits the tungsten grain size to 0.010 mm maximum when examined at 100X magnification. In addition the size of the copper filled areas are required not to exceed the tungsten grain size. Many times, strict adherence to this specification is both not possible and not critical. Once in a while, isolated copper filled areas slightly larger than the tungsten grain size do occur in the fabrication of the material. The material was accepted inasmuch as it is the only porous tungsten available without resorting to a porous tungsten development program. A typical area of the Sylvania tungsten-copper material specimen is shown in Figure 2-2, at a magnification of 100X. Note the larger size copper particles, scattered and isolated, within the tungsten matrix, which otherwise contains uniformily distributed, fine, copper particles.

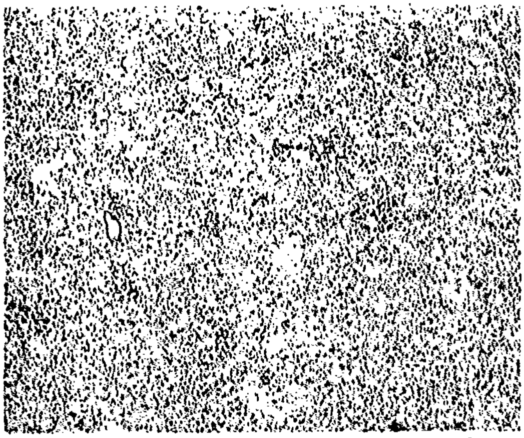

100X

Figure 2-2. 80%W-20% Cu as-polished. From Sylvania 1-inch diameter bar. Note the scattered larger size copper particles.

After machining the tungsten-copper nosetips to shape, the copper was extracted to arrive at the porous tungsten nose tips. Copper removal was performed in a vacuum furnace in which the samples were inductively heated to 2550°F in a 0.5 x 10^{-5} mm Hg vacuum. A total of four hours was required to melt and evaporate the copper. Prior to the evaporation process, and at intervals during the process, the samples were etched with a nitric acid-water solution to expedite the copper removal process. The etching process was used to remove the copper from the surface pores. The initial etch took 24 hours while subsequent etches, generally three in number, took 1/4 hour each. A summary of nosetip copper extraction results are shown in Table 2-II. A total of seven nosetip samples were prepared in this way. The weight loss in the specimen was due to the copper that was extracted and has been compared to the theoretical amount of copper that can be extracted. The amount of copper extracted varied between 8.75 to 12.47 percent of the original nosetip weight. A correlation between the amount of copper extracted from each particular nosetip and its performance in the 50 MW plasma arc tests could not be made. This confirms the evidence discussed later in this section, that the porous tungsten product achieved by purchasing tungsten-copper and extracting the copper results in nosetips lacking predictable reproducability in flow characteristics.

TABLE 2-II

Summary of Nosetip Copper Extraction Processing

Nosetip Model Number	Original Wt of Nosetip (grams)	Final Wt of Nosetip (grams)	Net Loss (grams)	Loss (Percent)	Theoretical Loss (Percent)
1	40.3102	35.2807	5.0295	12.477	11.4
2	41.09728	37.45972	3.63756	8.85	11.4
3	41.11572	36.22865	4.88707	11.88	11.4
4	41.76205	38.1075	3.654	8.75	11.4
5	40.00165	35.91087	4.09078	10.23	11.4
7	39.87619	35.71436	4.16	10.43	11.4
8	39.97719	36.35143	3.625	9.06	11.4

After extracting the copper from the tungsten nosetip materials, an investigation of each porous tungsten specimen was made in which optical microscopy, scanning electron microscopy (SEM), and X-ray microanalysis were used to locate and identify any defect areas. For each specimen, micrographs were taken of the upper threaded areas and a typical area on the conical section of the nosetip. No defects were found in any of these micrographs. In addition, for those specimens which were sputter coated with tungsten, micrographs of these areas were taken before and after coating. Typical of these are the micrographs taken on the sidewall of specimen number 4 which are shown in Figures 2-3, 2-4, 2-5 and 2-6.

A vapor deposited coating with 3μm of tungsten produced the morphology shown in Figures 2-5 and 2-6.

Typical micrographs of the blind holes taken on specimen number five are shown in Figures 2-7, 2-8, 2-9 and 2-10.

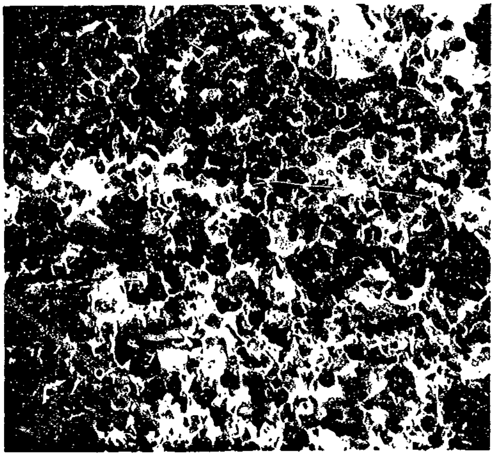

500X, 20KV, 0°

Figure 2-3. Typical Area on the Cap of Specimen No. 4

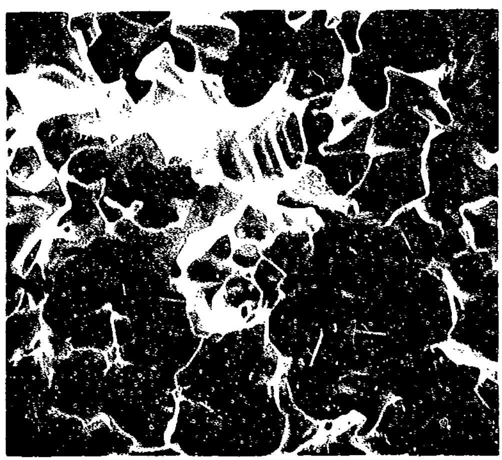

2000X, 20KV, 0°

Figure 2-4. Surface at the Center of Figure 2-3

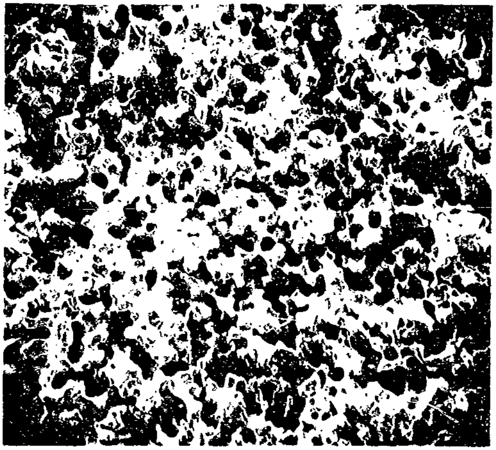

500X, 20KV, 0°

Figure 2-5. Typical Area on the Cap of Specimen No. 4 after Sputter Coating with 3 Microns of Tungsten

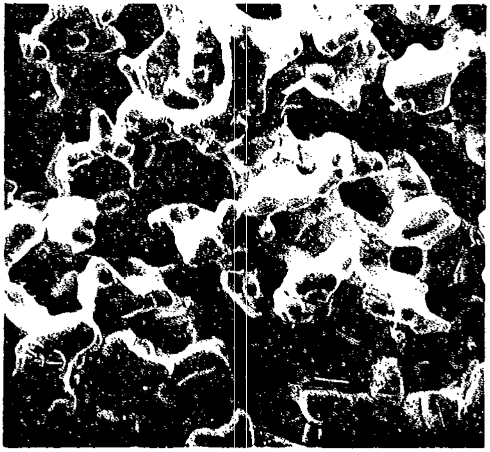

2000X, 20KV, 0°

Figure 2-6. Coated Surface at the Center of Figure 2-5

12X, 10KV, 22°

Figure 2-7. Blind Holes on the Tip of Specimen No. 5

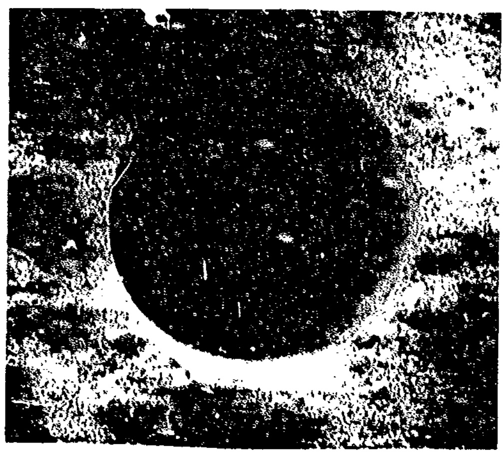

100X, 20KV, 22°

Figure 2-8. Blind Hole at the Center of Figure 2-7

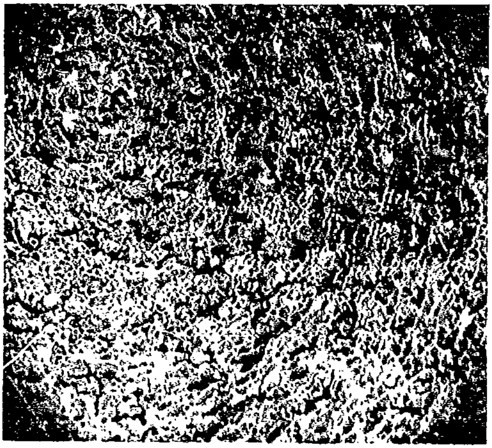

500X, 20KV, 22°

Figure 2-9. Area at the Bottom of the Hole in Figure 2-8

2000X, 20KV, 22°

Figure 2-10. Surface at the Center of Figure 2-9

2.1.3 Sealing of Nosetip Model Threads

Prior to the assembly of the nosetips and the model holder, the threads in the porous tungsten nosetips had to be sealed externally to ensure that the coolant would not leak through the threads and provide a lower pressure path than the nosetip itself. The threads were gold plated. Immediately prior to assembly, silicone rubber was applied to the threads. The seal was preserved with the combination of the gold plating and the silicone rubber. During the gold plating process, the sphere cone portion of the nosetip was covered with a neoprene rubber plating shield. The process used for gold plating the threads on each porous tungsten nosetip is as follows:

1 The part was ultrasonically cleaned for 2 minutes in a 20 percent solution of Brulin 815XM.

2 The part was rinsed in running water for 2 minutes and in deionized water for 1 minute.

3 The electrical circuit was activated for 30 seconds while the part was dipped in a solution of 20 percent HF plus 20 percent HNO at 130 degrees F.

4 The part was double rinsed in deionized water, and subsequently neutralized for 10 seconds in a 5 percent solution of Na OH.

5 The part was immediately placed (without rinse) into a gold bath, where it was electroplated for 72 minutes at 1 volt dc.

6 The part was thoroughly rinsed in cool running water for approximately 3 minutes.

7 The part was immediately dried with clean filtered air and sealed in a fresh plastic bag.

The holding fixture used for the electroplating process is schematically shown in Figure 2-11.

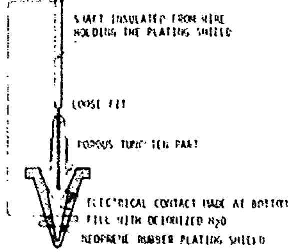

Figure 2-11. Holding Fixture for Electroplating Porous Tungsten Part with Gold to Seal Pores

2.2 Model and Holder Configuration Design and Analysis

2.2.1 Model and Model Holder Design

The model and model holder assembly design is shown in Figure 2-12. The nosetip (Figure 2-1) is machined from tungsten-copper (80W/20Cu) as previously described, from which the copper is extracted, leaving a porous tungsten matrix. The nosetip is held into the model adapter forward body by a threaded appendage. A high pressure liquid coolant seal is provided by an O-ring at the tip of the appendage.

The model adapter forward body is shown in Figure 2-13. It was machined from tungsten-copper and includes female threads to adapt to the nosetip and to the model adapter aft body. An O-ring provides a high pressure seal at the interface with the aft body. The model adapter aft body, shown in Figure 2-14, is machined from 347CRS. The forward end features a male thread to adapt to the model adapter forward body. The aft end is threaded to receive a 1-inch adapter which holds the assembly to the sting. Forward of the 1-inch thread, the internal passage is tapped for 1/4-inch NPT. This thread adapts to the coolant conduit. Both sections of the model adapter were wrapped with a silica phenolic heat shield.

The coolant conduit shown in Figure 2-15 is machined from 5/8-inch Type 304CRS tubing. Both ends are threaded 1/4-inch NPT. The forward end mates with the model adapter aft body. The aft end threads into an elbow. A hexagonal cross section is machined into the conduit near the aft end to provide a means for holding it while tightening the elbow on the aft end. A centering washer (Figure 2-16) positions the conduit in the tunnel through the sting.

The entire assembly was mounted in the Wright-Patterson Plasma Arc Facility sting. Fully machined parts are shown in Figures 2-17 and 2-18.

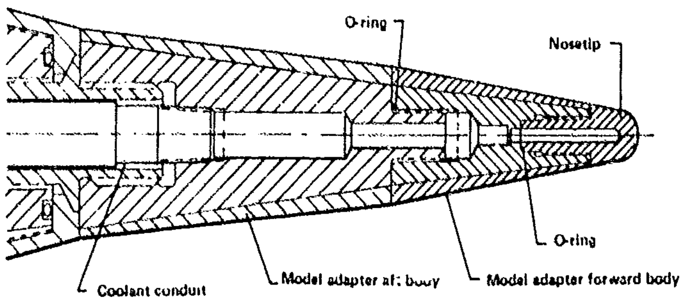

Figure 2-12. Model and Model Holder Assembly

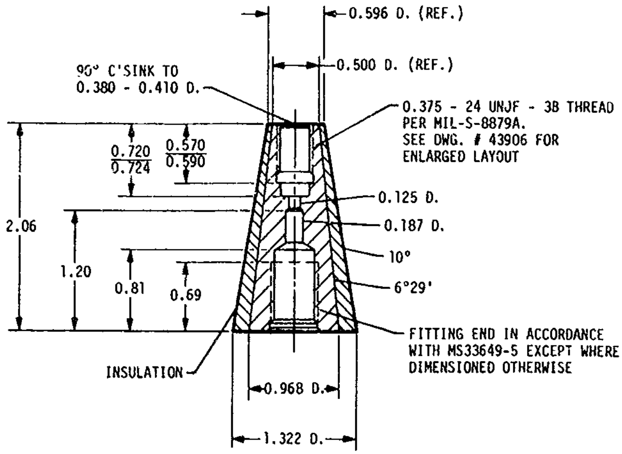

Figure 2-13. Model Adapter Forward Body

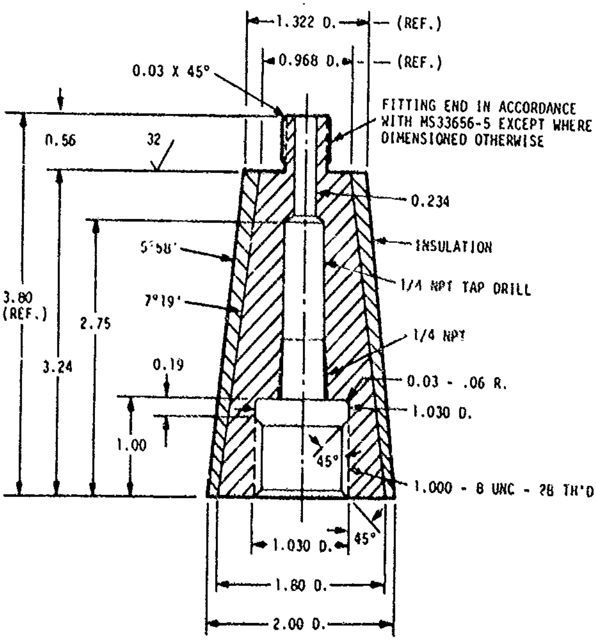

Figure 2-14. Model Adapter Aft Body

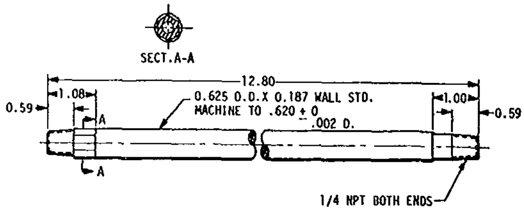

Figure 2-15. Coolant Conduit

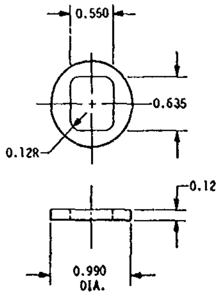

Figure 2-16. Centering Washer

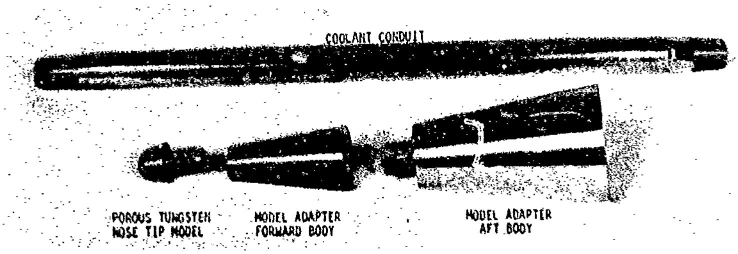

Figure 2-17. Model and Model Holder (Exploded)

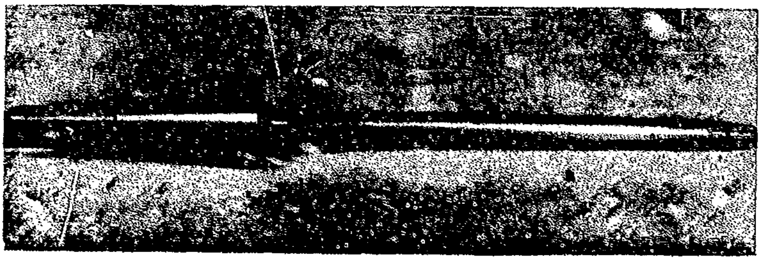

Figure 2-18. Model and Model Holder (Assembled)

2.2.2 Stress Analysis

The final model holder design evolved through a study of the response to aerodynamic loads, thermal stress, and internal pressures which the system would experience in the 20 atm tests at the Wright-Patterson 50 MW Plasma Arc Facility. The design configurations evaluated are shown in Figure 2-19. In the final analysis, the thermal stress response of the system was the most critical factor in arriving at a final design.

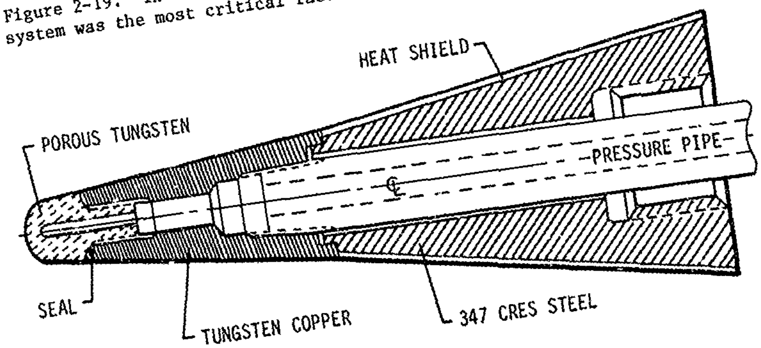

a. INITIAL DESIGN CONCEPT

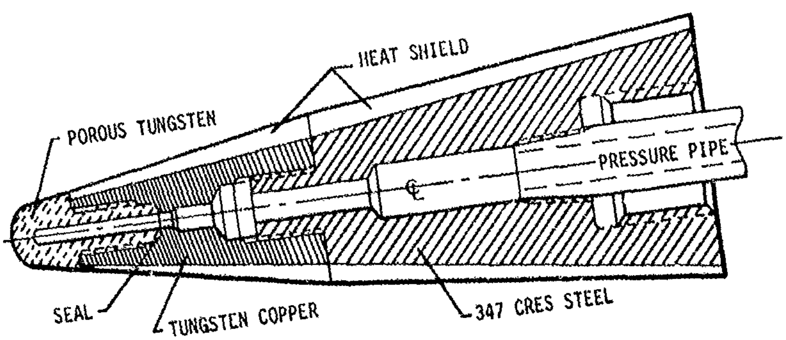

b. FINAL DESIGN

Figure 2-19. CONAP Design Configuration

The structural design requirements due to aerodynamic loads were based on the environments which the CONAP models experience upon insertion into the plasma arc stream facility (References 10 and 11). The CONAP specimens are mounted on a rack which is moved laterally into the plasma arc stream. To assess the air loads, it was assumed that the test specimen could move into the stream with a velocity of 100 ft/s. This resulted in an effective angle of attack of 1/2 degree. Using hypersonic aerodynamic relations, the running load and the overall shear and bending moment diagrams were developed for the worst case (80 atm) condition. These are shown in Figure 2-20. The stresses in the test specimen, resulting from these loads, were determined to be insignificant.

A three-dimensional thermal response analysis of the initial design concept shown in Figure 3-9 was used as the basis for the thermal stress and internal pressure analysis (Reference 12) of the porous tungsten nosetip and the tungsten-copper model holder. The tungsten-copper material properties are based on Reference 9.

In the infiltrated material the copper does not bond to the tungsten-copper matrix and does not add to the tensile strength of the tungsten-copper material. For the purposes of this analysis, it was assumed that porous tungsten strength is an inverse function of porosity, and therefore, porous tungsten tensile strengths equal to 80 percent of the tungsten-copper values were considered reasonable. The material properties used are shown in Figure 2-21.

The results of the thermal stress analysis of the tungsten-copper model holder in the 20 atm environment are shown in Figure 2-22. It can be seen that in the aft portion of the model (Figure 2-22a) that the thermal stress exceeds that allowable after 5.1 seconds. Thermal stresses at points forward of the aft section did not exceed that allowable.

The results of the thermal stress analysis at the 80 atm environment are shown in Figure 2-23. Here, it can be seen that at two rearward points checked, thermal stresses exceeded that allowable after 1.25 seconds. The stresses in the forward portion, which is a thinner section, did not exceed that allowable. The thermal stress analysis of the initial tungsten-copper model holder, Figure 2-19, limits the test time to 5.1 seconds for the 20 atm condition and 1.25 seconds for the 80 atm condition.

Hoop stress and a thread shear strength analyses were conducted on the shaft of the nosetip. The analysis considered a 5000 psi internal pressure. These are summarized in Figures 2-24a and 2-24b, respectively. These curves show that a safety factor of 2.0 can be maintained on the hoop stress and a safety factor of 3.0 on the thread shear if the 20 atm test is limited to 4 seconds and the 80 atm test is limited to 2 seconds.

Based on these limitations, the final design (Figure 2-19b) incorporated a heat shield over the entire steel and tungsten-copper bodies. This significantly reduced the temperatures and resulted in thermal stresses and hoop stresses no longer being critical. In addition, to maximize the safety factor for the porous nose threads, a seal was placed aft of the thread to minimize tension force, and a radius root thread was used to decrease the stress concentration.

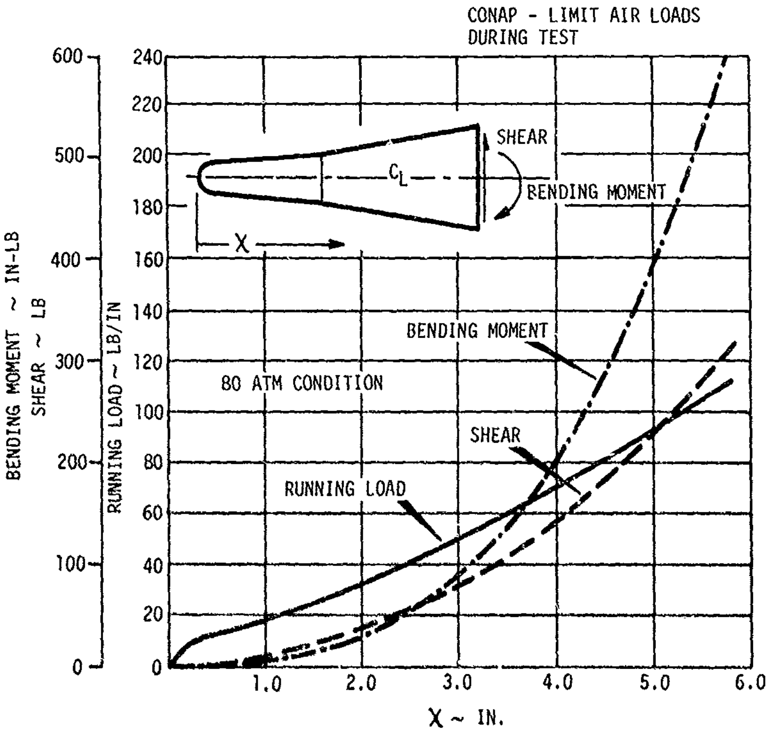

Figure 2-20. Overall Test Specimen Airloads

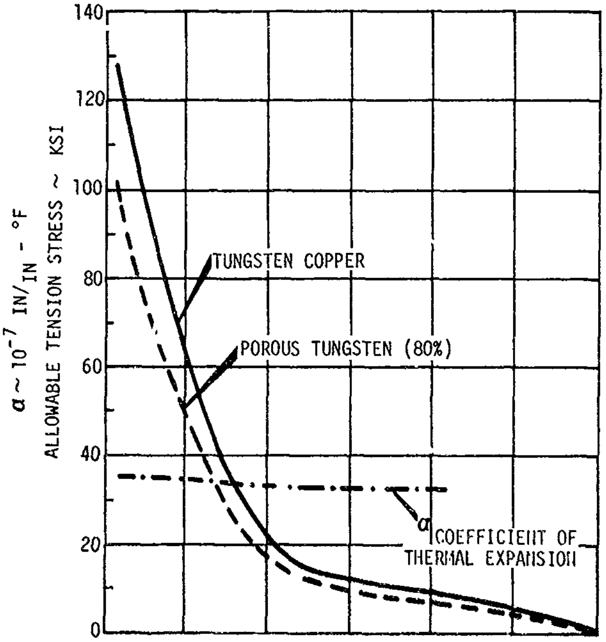

a. Allowable Stress Versus Temperature
α Versus Temperature

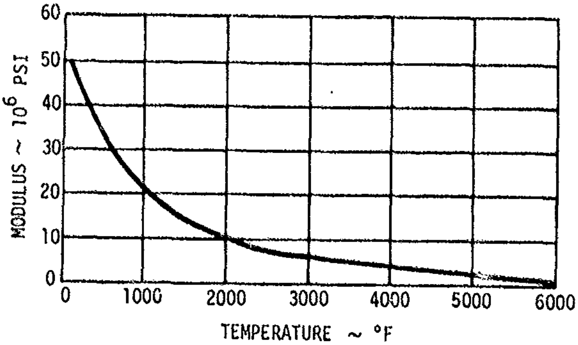

b. Tungsten Copper and Porous Tungsten

Figure 2-21. Material Properties

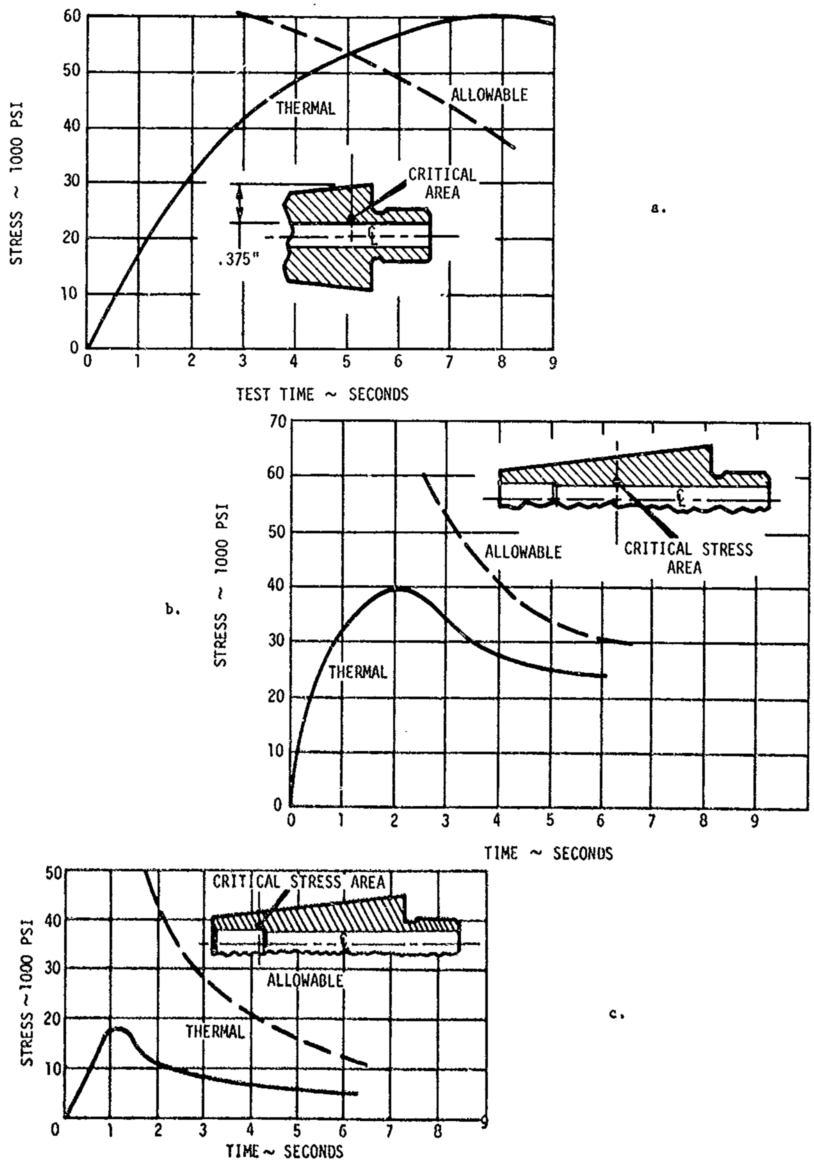

Figure 2-22. Critical Thermal Stress of Tungsten-Copper Body-Initial Design Concept of 20 Atm Test Condition

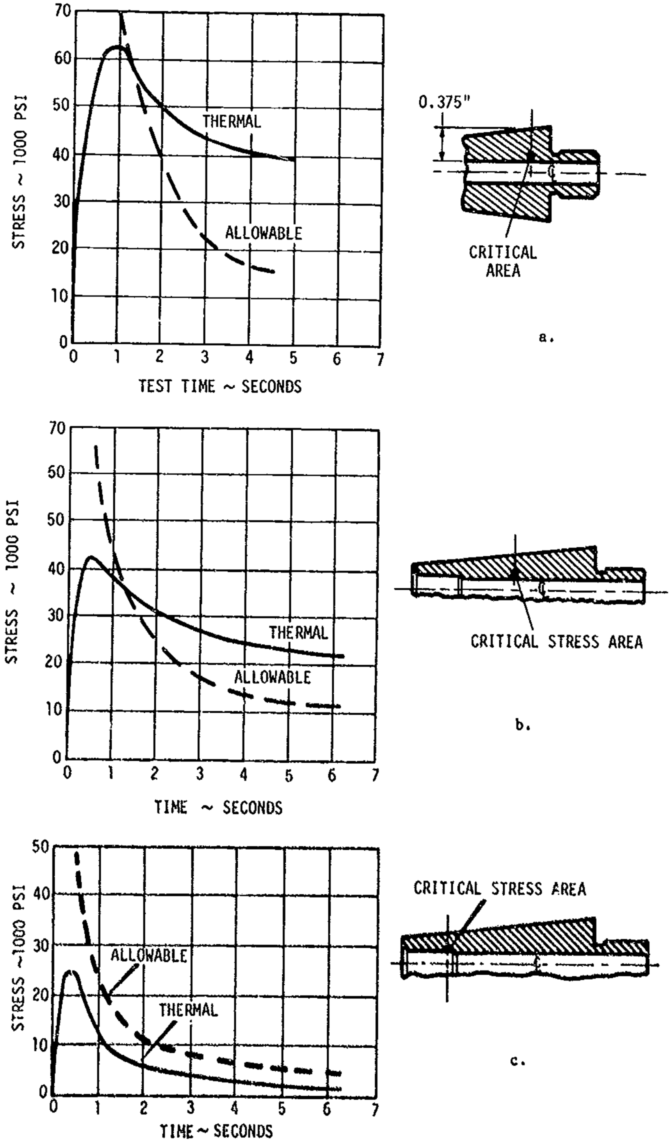

Figure 2-23. Critical Thermal Stress of Tungsten-Copper Body-Initial Design Concept of 80 Atm Test Condition

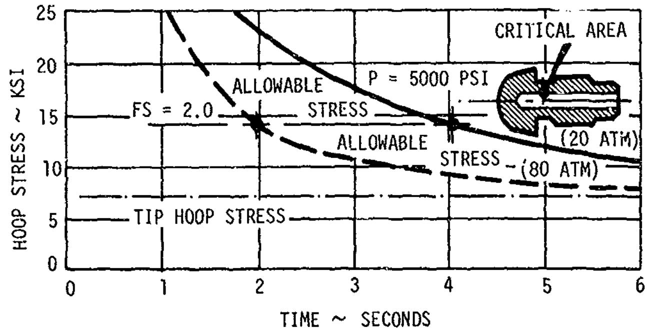

a. Critical Hoop Stress

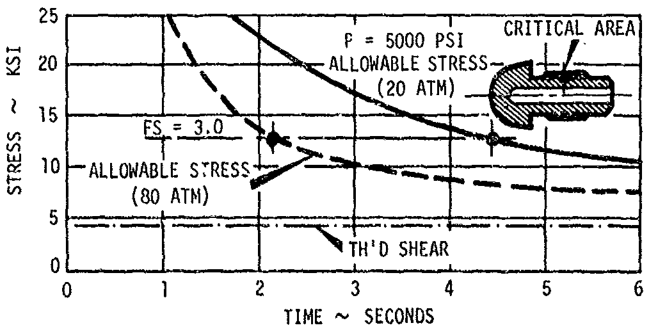

b. Critical Thread Stress

Figure 2-24. Porous Tungsten Nose Critical Stresses

2.3 Plasma Arc Test Conditions and Geometry

The CONAP porous tungsten matrix concept was evaluated at the Wright-Patterson 50 MW Plasma Arc Facility, RENT Leg, at the 20 atm pressure condition. Table 2-III describes the model geometry and the desired test conditions. Prior to testing, it was assumed that the internal shroud nozzle hardware (Reference 11) would be implemented. However, immediately prior to the test series due to higher priority facility considerations the hardware was removed, which slightly altered the test conditions. The nosetip environment data were obtained by a copper calorimeter model identical in configuration to the nosetip, in which three calorimeters were imbedded. A copper pressure model, with a similar configuration, had pressure taps at the same locations as the calorimeters. Pyrometers used during the tests to record surface temperature were aimed so that their viewing area coincided with the location of the calorimeters on the calorimeter model. Data from these instruments were processed to provide heat flux, surface pressure, and temperature distributions.

TABLE 2-III

Model Geometry and Desired Test Conditions

Model	Nose Radius (RN, Inches)	Cone Half Angle (degrees)	P_{t_2} ℄ x = 0.1" (atm)	Mach No. x = 0.1 in.	q Stag (BTU/ft²-s)	H ℄ (BTU/lb)
CONAP	1/4	10	20	2.0	3500	2800
Pitot	1/4	6	20	2.0	3500	2800
Calorimeter	1/4	6	20	2.0	3500	2800

2.4 Test Matrix for the 20 Atm Tests

The test specimens incorporated several variations of the basic model (Figure 2-1). An optimum nosetip would control distribution of the coolant flow to correspond to the heat flux distribution. As described in Section 2.1.1, two different techniques were employed in an attempt to achieve ideal flow distribution. One technique was to drill blind holes on the exterior surface of the spherical portion of the nosetip to decrease pressure drop in this region, thus increasing the local flow rate of the coolant. The other technique was to vapor deposit tungsten on the conical surface of the nosetip to increase the pressure drop in this region, thus decreasing the local flow rate of the coolant. The thickness and extent of the vapor coating were varied to control the flow distribution. The test specimens employed various combinations and degrees of these two techniques.

The original test plan included the configurations shown in Table 2-IV. The sequence and selection represented a logical progression in the flow modification methods from test to test so they could be adequately evaluated in their contribution to the nosetip performance. This plan, however was not strictly followed (as will be shown later) because the actual modifications to specimen flow characteristics proved to be much smaller than the unanticipated specimen to specimen variation.

TABLE 2-IV

Test Plan for the 20 atm Test Condition

Model Number	Material	Description of Flow Modifications	CONAP Plenum Pressure (psi)	Test Time (seconds)	Model Configuration
2	Porous Tungsten	None	2000 1750 1500 1250	1 1 1 1	
3	Porous Tungsten	1μ sidewall vapor deposit	2000 1750 1500 1250	1 1 1 1	
4	Porous Tungsten	3μ sidewall vapor deposit	2000 1750 1500 1250	1 1 1 1	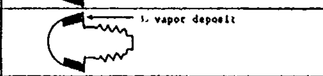
8	Porous Tungsten	5μ sidewall vapor deposit	2000 1750 1500 1250	1 1 1 1	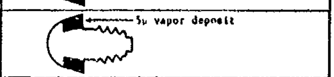
5	Porous Tungsten	3μ vapor deposit on sidewall Blind holes	2000 1750 1500 1250	1 1 1 1	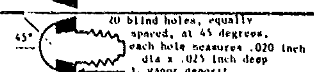
7	Porous Tungsten	0.025 inch depth sonic Pt blind holes 5μ vapor deposit on sidewall	2000 1750 1500 1250	1 1 1 1	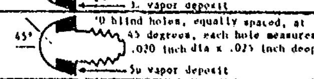
9	Tungsten Copper	Discrete holes 0.03 inch dia	1000 800 700 600	1 1 1 1	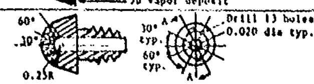

2.5 Model Installation

Prior to installation the model and model holder assembly, as shown in Figure 2-12 were assembled and leak checked to 5000 psi pressure. As a part of the final sealing and leak check operation immediately prior to testing at the 50 MW Plasma Arc Facility, sufficient data were taken so that average flow characteristics (permeability and inertial resistance coefficient) could be determined for each nosetip. The assembly was then installed in the sting using the 1-inch threaded adapter to hold the assembly in position. The centering washer (Figure 2-16) was placed over the hexagonal section on the aft end of the coolant conduit (Figure 2-15), and an elbow was threaded onto the aft end of the conduit. The hexagonal section was used to hold the conduit while the elbow was tightened. The elbow was positioned to point downward by rotating the entire assembly on the 1-inch adapter. Additional plumbing was then attached to the elbow to connect to the coolant manifold. Finally, the aft cover was placed on the sting.

A coolant manifold with a solenoid valve in each of the two branches directed coolant flow to either of the two test specimens mounted on the 50 MW test carriage. The control system for the coolant expulsion system had two timers which were set to provide timed sequencing of the two manifold valves and also to provide timed sequencing of the four flow control valves so that the coolant flow could be decreased in discrete steps during the exposure of each specimen. The flow rate/time sequence was adjusted for each separate model as required. The timers also provided the switch of flow from one model to the next model commensurate with the carriage timing sequence.

2.6 Instrumentation

Two instrumented models were fabricated to evaluate conditions in which each test model was exposed in the plasma arc. These two models, built by Aerotherm/Acurex, are shown in Figure 2-25. The model on the left is a calorimeter model containing three calorimeters. One is located at the stagnation point, one at a point 50 degrees around the spherical nose from the stagnation point, and the third is 1/4 inch aft of the tangency point between the spherical nose and the conical forebody. The model on the right in Figure 2-25 is a pressure model. Static pressure ports are located at positions corresponding to those described for the calorimeters. The aft location is shown clearly in Figure 2-26. These two models were mounted on stings similar to those on which the test models were mounted. The aft faces of these models were designed to interface with an adapter which was a part of the 50 MW Plasma Arc Facility. The two instrumented models were swept through the plasma jet at a controlled rate during each test run to provide heat flux and pressure distribution data.

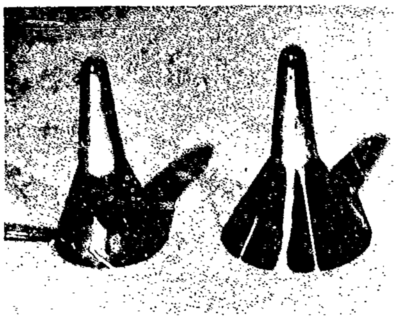

Figure 2-25. Instrumented Plasma Arc Models

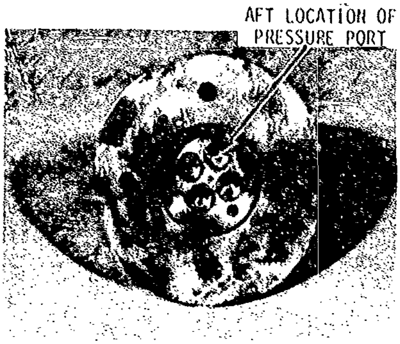

Figure 2-26. Aft End of Pressure Probe

Instrumentation used to measure coolant pressure and coolant flow rate included a venturi, two pressure transducers, and a thermocouple. The arrangement of the venturi and transducers used is given in Appendix I. Digital volt meters were employed to monitor the coolant absolute pressure and the differential between the absolute pressure and the venturi throat pressure. An iron constantan thermocouple was attached to the stainless tubing just upstream of the coolant delivery hose. This junction was thermally insulated to provide a reasonably accurate thermocouple response to the liquid coolant temperature. A summary of the instrumentation used during the tests is shown in Table 2-V.

TABLE 2-V

Instrumentation and Equipment Requirements

Measurement	Range	Data Source	Instrumentation Required
Coolant temperature	0 to 80°F	Iron constantan thermocouple attached to 3/8 inch stainless tube on coolant supply cart, externally insulated	Strip type recorder or step type printer
Coolant absolute pressure	0 to 5000 PSIA	Absolute pressure transducer located on coolant supply cart, Statham model PA822-5M	Digital volt meter (monitor) 15 volt power supply Bridge conditioner Wide band amplifier Oscillograph Ambilog hybrid computer
Venturi differential pressure	0 to 500 PSID	Differential pressure transducer located on coolant supply cart, Statham model PL280-TC-500-350	Digital volt meter (monitor) 15 volt power supply Bridge conditioner Wide band amplifier Oscillograph Ambilog hybrid computer
Stagnation point pressure distribution	Stag point-0 to 300 PSIA 50° point - 0 to 150 PSIA Body point-0 to 50 PSIA	Pressure Model Statham transducer PA285TC-500 Statham transducer PA285TC-150 Statham transducer PA285TC-50	15 volt power supplies Bridge conditioners Wide band amplifiers Oscillograph Ambilog hybrid computer
Surface heat flux distribution	Stag point 3600* 50° point 1700* Body point 350* *BTU/ft²-s-°F	Calorimeter model	Bridge conditioners Wide band amplifiers Oscillograph Ambilog hybrid computer
Nose tip surface temp distribution	Stag point 2000-3000°R 50° point 1500-2000°R Body point 1000-1500°R	3 optical pyrometers with a field of view of 0.06 to 0.10 inch	That required for recording output from 3 pyrometers
Weight of ammonia cylinder	0 to 300 lb	Beam type platform scales	–

2.7 Test Conditions

Test conditions were measured for each run by the pressure model and the calorimeter model. The data from run to run showed excellent agreement. Figure 2-27 shows the pressure data for the three runs. Pressure data were taken at three discrete locations. As shown in Figure 2-27, the pressure distribution follows the Modified Newtonian approximation quite well. The heat flux distribution data are shown in Figure 2-28. Calorimeters were located at the same axial downstream distances as the pressure taps on the pressure model. The heat flux data taken for the three runs also showed excellent agreement. The heat flux data also agreed well with the cos 3/2 θ distribution which suggests, according to Reference 13, that laminer flow existed over the total calorimeter model. Table 2-VI summarizes the nominal facility conditions during this test series. The enthalpy is calculated from a modified version of the Faye-Riddell heat transfer equation adapted to the 50 MW facility, (Reference 14) and requires heat flux and stagnation pressure as input data. A comparison of Tables 2-III and 2-VI shows that the test conditions, in particular the stagnation enthalpy, were more severe than specified prior to the test.

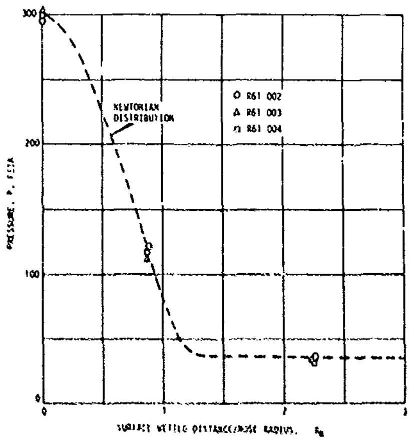

Figure 2-27. Pressure Distribution

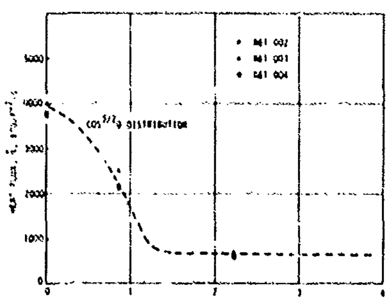

Figure 2-28. Heat Flux Distribution

TABLE 2-VI

CONAP Testing at Wright-Patterson AFB Dayton, Ohio

Test Conditions:	
$q_{STAG\ NOM}$	= 4000 BTU/ft^2-s
H_{STAG}	= 3800 BTU/lb
P_{STAG}	= 20 atm

2.8 Porous Tungsten Nosetip Flow Characteristics

Testing in the 50 MW Plasma Arc Facility was conducted on porous tungsten models which were assembled, sealed, and leak checked immediately prior to shipping the models to the facility. During the leak check operation, data were taken at room temperature with nitrogen gas to evaluate the average flow characteristics of each nosetip. Analysis of these data showed that of the nosetips fabricated, only one (nosetip No. 3) possessed the flow properties that were identified as desired properties as defined by Reference 1 and were anticipated to exist in the nosetip. A comparison of porous tungsten flow characteristics is shown in Figure 2-29. The cross-hatched area possesses desired porous tungsten nosetip flow characteristics. This was based upon the analysis of Reference 1. The materials whose flow characteristics lie within the cross-hatched area are the 80 percent Sylvania and 80 percent Wah Chang materials. Although the 80 percent Sylvania porous tungsten material was used exclusively in the current test series, the flow characteristics for the nosetips fabricated from this material showed significant scatter as well as a large departure from the range of desired properties. Only nosetip No. 3 possessed flow properties that were anticipated before the tests. Nosetip model No. 2, which contained no flow modifying additions, required the highest coolant pressure to achieve a given amount of flow, and was not used. If these nosetips were ranked in terms of the amount of pressure required to push a given flow rate through the matrix, nosetip No. 2 would require the highest upstream pressure, followed by nosetip 4, 5, 8 and 7. Finally, nosetip No. 3 required the least upstream pressure of this group. Therefore it can be seen that the scatter in the basic flow properties of the nosetips, even though they were all from the same batch of material, appears to overshadow the nosetip modifications originally made to study the effects of these modifications on the control of flow distribution in the nosetip matrix.

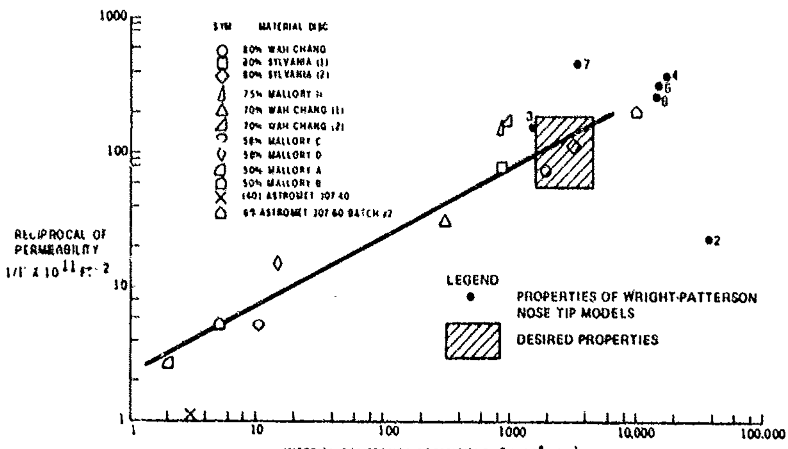

Figure 2-29. Porous Tungsten Flow Characteristics Correlation and Materials Assessment

2.9 Test Results

The models shown in Figure 2-30 were all tested in the identical 20 atm environment. Table 2-VII summarizes the test results. All tests were initially intended to run for a total of 4 seconds. The first run consisted of model No.'s 7 and 8 manifolded to the supply source. Model No. 7 was located on strut No. 1 and model No. 8 was located on strut No. 3 with strut No. 2 being left empty. The expulsion system (see Appendix I) provided coolant first to the model on strut No. 1 and subsequently to the model on strut No. 3. During the first run, model No. 7 split longitudinally at 0.5 second after reaching centerline. This model was not recovered. During the remaining 3.5 seconds that the model holder for model No. 7 was at centerline, the expulsion system vented through the relatively large orifice that was opened. Thus, when model No. 8 entered the flow field, coolant pressure was very low and supplied insufficient coolant. The model, therefore, ablated and eventually exposed the internal hole. Figure 2-31 shows the post test condition of model No. 8.

The second run consisted of models 4 and 5; model No. 4 was on strut No. 1 and model No. 5 was on strut No. 3. Both of these models were successful and survived for the full 4-second duration. Model No. 4 had a small amount of stagnation point ablation and no known matrix cracking. A post test view of model No. 4 is shown in Figure 2-32.

Model No. 5, however, developed a large crack on the sidewall near the end of the 4-second test, causing the gas to vent through the crack and thereby starving the stagnation region. A post test view of model No. 5 is shown in Figure 2-33.

The third test consisted of model No. 3 and model No. 9. Model No. 3 was placed on sting No. 1 and model No. 9 on sting No. 3. Model No. 3 broke at the neck 1.2 seconds after reaching centerline. The data showed that up until that point, the nosetip was performing well. Figure 2-34 shows a post test photograph of the model No. 3. The surface blemishes are due to the spherical nosetip impacting and scraping several metallic surfaces after being propelled by the pressures in the plasma arc. The tip was later found downstream of the plasma arc ejector. Because model No. 3 broke at the neck and broke away from the model holder, the expulsion system vented similarly as in the first test. As model No. 9 reached centerline supply pressure of the ammonia was roughly 20 atm which was equal to the stagnation pressure of the facility. Thus, the sideports had pressure differential whereas the stagnation point did not. The model ablated at the stagnation region and exposed the internal supply orifice. It is interesting to note that once the central flow passage was uncovered, ablation ceased, even with inadequate coolant (Figure 2-35).

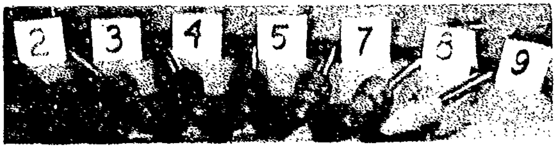

Figure 2-30. Various Models Fabricated for Testing in the 50 MW Test Facility

TABLE 2-VII

Test Results at Wright-Patterson 50 MW Plasma Arc

	Model No.	Description	Results	Model Condition
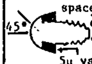 20 blind holes equally spaced at 45 degrees each hole 0.02 inch dia x 0.025 inch depth; 45°; 5μ vapor deposit	7	Porous tungsten 5μ tungsten on sidewall Blind holes	• Model split longitudinally at 0.5 seconds	• Not recovered
 5μ vapor deposit	8	Porous tungsten 5μ tungsten on l sidewall	• Low pressure flow to this model because strut no. 1 model vented • Ablated to expose internal hole	• Longitudinal crack on sidewall
 3μ vapor depot	4	Porous tungsten 3μ tungsten on sidewall	• Survived for total test time of 4 seconds • Small amount of ablation at stagnation point	• No longitudinal cracking • No known subsidiary cracks
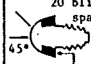 20 blind holes equally spaced at 45 degrees each hole 0.02 inch dia x 0.025 inch depth; 45°; 3μ vapor deposit	5	Porous tungsten 3μ tungsten on sidewall Blind holes	• Survived for total test time of 4 seconds • Gas vented through crack near end of test and starved stagnation point and blind hole area	• Longitudinal crack • Subsidiary cracks
 1μ vapor deposit	3	Porous tungsten 1μ tungsten on sidewall	• Broke at neck at 1.2s test time • Data showed that nose tip was working well	• Nose tip in good shape
 60°; 30°; 0.025R; A; 30°; 60°; A; Drill 13 holes 0.020 dia	9	Tungsten-Cu Discrete holes	• Supply pressure roughly equal to stagnation pressure of facility (20 atm) • Ablated at stagnation point and exposed internal hole	• Ablation ceased when internal hole was exposed

Test conducted at:
H_{STAG} = 3800 Btu/lb q_{STAG} = 4000 Btu/ft^2-s
P_{STAG} = 20 atm Test time = 4 seconds

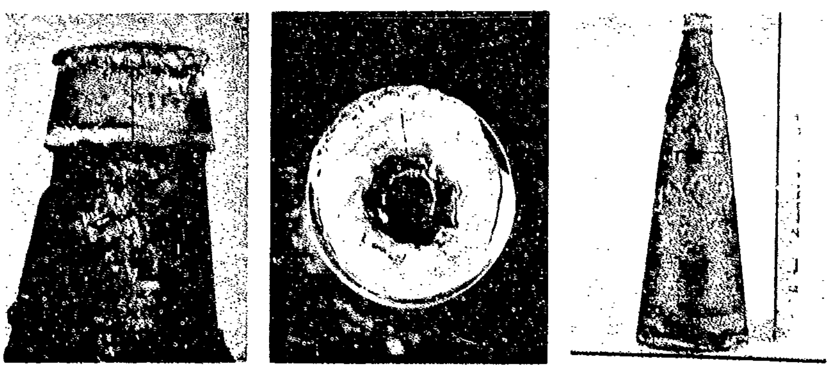

Figure 2-31. Post Test of Porous Tungsten Nosetip No. 8 Supplied With Inadequate Coolant and Tested for 4 Seconds

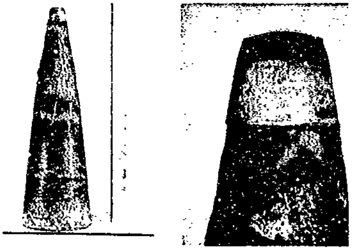

Figure 2-32. Post Test of Porous Tungsten Nosetip No. 4 Tested for 4 Seconds

Figure 2-33. Post Test of Porous Tungsten Nosetip No. 5 Tested for 4 Seconds

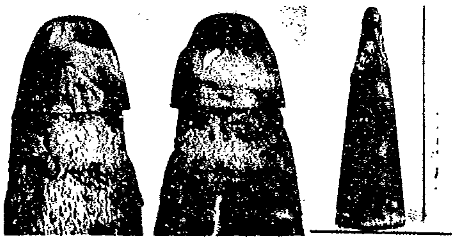

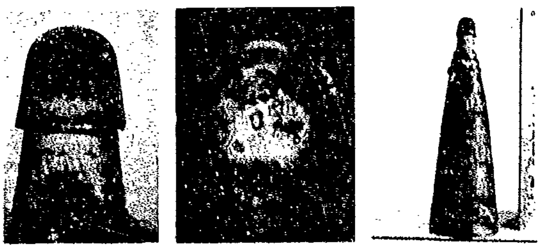

Figure 2-34. Post Test of Porous Tungsten Nosetip No. 3 Tested for 1.2 Seconds

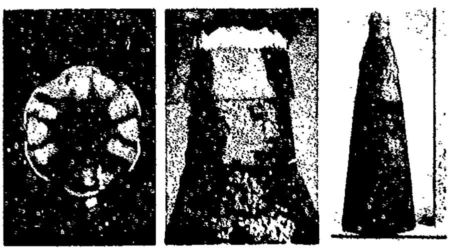

Figure 2-35. Post Test of Discrete Hole Nosetip with Inadequate Coolant

Figures 2-36, -37, and -38 show pyrometer data for the stagnation point region, the 50-degree point on the spherical tip, and the conical point on the body 1/4 inch aft of the tangency point. It is interesting to note that in Figure 2-38, both nosetip No. 5 and nosetip No. 9 appeared to have very high surface temperature at the sonic point. It can be construed that the discrete holes and blind holes induce local sonic point turbulence, thereby causing higher heating and temperature at this location. From Figure 2-37, it can be seen that the sidewall temperature of nosetip No. 3 was indicating far more coolant emerging from the sidewall than the other nosetips. This is expected in light of the flow characteristics of this nosetip when compared to others. Flow rates to the models are shown in Figure 2-39.

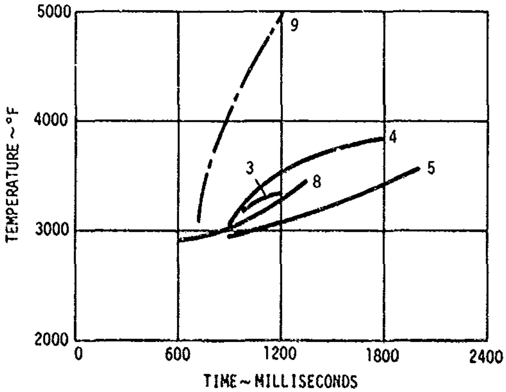

Figure 2-36. Stagnation Point Temperature

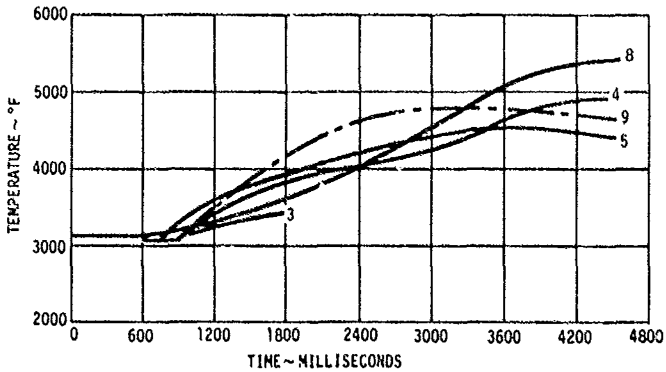

Figure 2-37. Sidewall Temperature (1/4 Inch Aft of Tangency Point)

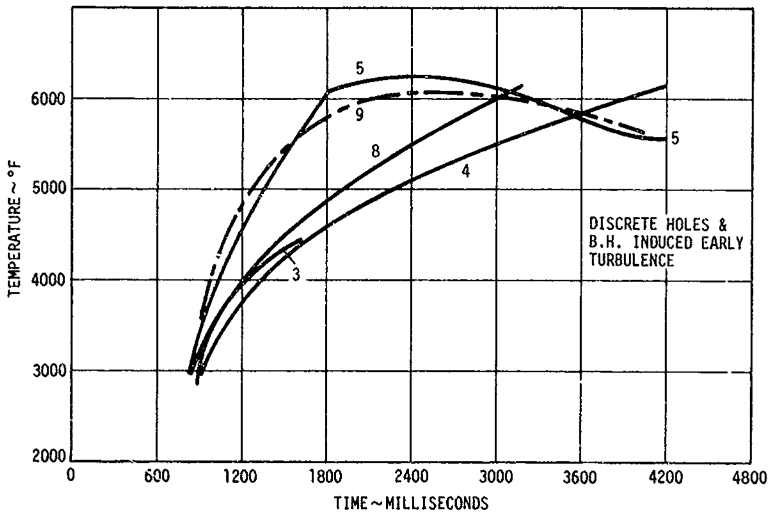

Figure 2-38. Surface Temperature at the 50-Degree Location on the Sphere

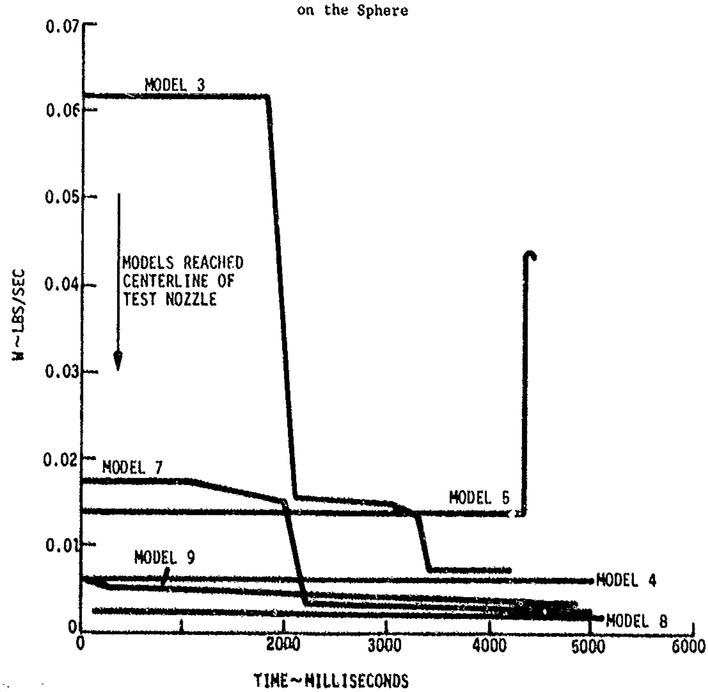

Figure 2-39. Model Flow Rate History at the 50 MW Plasma Arc Facility

3.0 RAMBURNER TEST PROGRAM

Testing was conducted in the Martin Marietta Ramburner Facility on surrogate nosetips made from aluminum to assess the configurational characteristics of several CONAP discrete hole matrix concepts. These simulated hot-gas tests evaluated survivability of several nosetip configurations under conditions scaled to an advanced interceptor flight condition. The test series in the ramburner facility was conducted at zero-degree angle-of-attack; however, flow visualization was obtained on each concept both at zero-degree and 10-degree angles-of-attack.

Five configurations were evaluated and are summarized in Figure 3-1 and described in detail in Figures 3-2 through 3-6. The configurations include those with one centerline hole and those with one centerline hole and side-slots. Prior to testing these configurations to determine minimum survival flow rates, flow visualization work in the cold flow facility verified that flow emanates from the sideslots as well as the centerline hole at both zero and 10-degree angle-of-attack as shown in Figure 3-7. The flow visualization tests were conducted in Martin Marietta's Cold Flow Facility adjacent to the Ramburner Facility. The Cold Flow Facility is a simple Mach 2.5 free-jet nozzle connected to an upstream high pressure nitrogen supply. It is used primarily for flow visualization and pressure distribution tests.

The Ramburner test conditions are summarized in Table 3-I. The models were tested for 10 seconds in each run and were mounted on a conical sting shown in Figure 3-8. The models were tested several times with flow rates to each model being initially high and then sequentially reduced from run to run until the model failed in order to determine relative performance. Table 3-II through 3-VI detail the tests conducted on each model. Table 3-VII summarizes and compares the overall test results.

Two of the configurations tested have merit: 1) the 30-degree ogive with slots and 2) the sphere-cone-cone with slots. These models required the least amount of coolant at zero angle-of-attack to survive. For these concepts to have merit in future flight test programs, these results would have to be verified for a range of angle-of-attack conditions to show that these configurations remain optimum at all appropriate angles-of-attack.

CONFIGURATION NUMBER	CONFIGURATION		DESCRIPTION
1		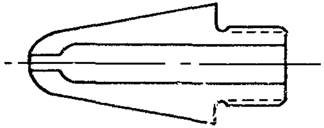	SPHERE-CONE WITH 1/8-INCH CENTERLINE HOLE
2	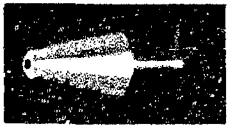	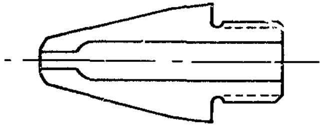	SPHERE-CONE-CONE WITH 1/8-INCH CENTERLINE HOLE
3		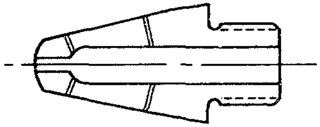	SPHERE-CONE-CONE WITH 1/8-INCH CENTERLINE HOLE AND SIDESLOTS
4	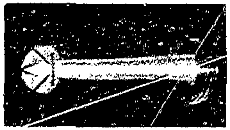	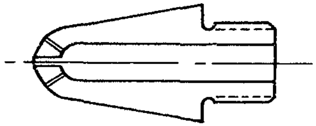	60-DEGREE BICONIC WITH 50-MIL CENTERLINE HOLE AND SLOTS
5	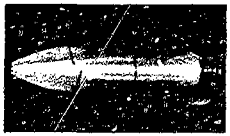	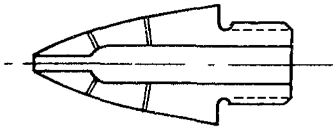	30-DEGREE OGIVE WITH 1/8-INCH CENTERLINE HOLE AND SIDESLOTS

Figure 3-1. CONAP Discrete Hole Configuration Tested in Ramburner

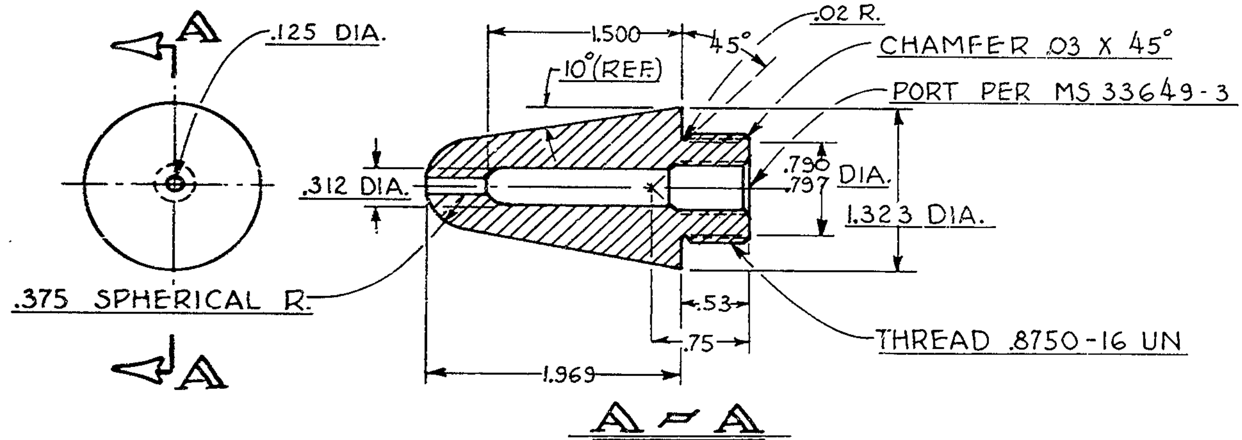

Figure 3-2. CONAP Discrete Hole Configuration 1

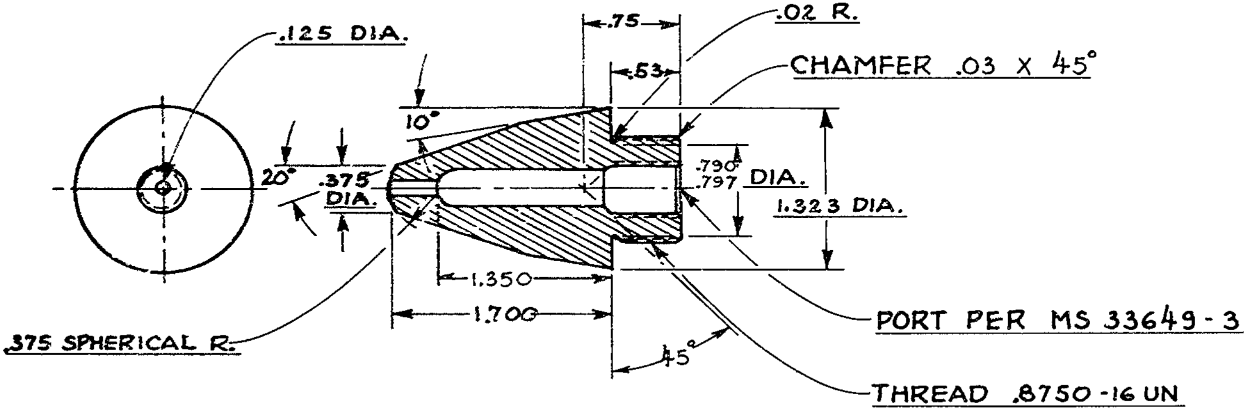

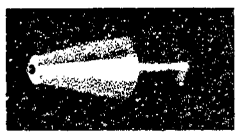

Figure 3-3. CONAP Discrete Hole Configuration 2

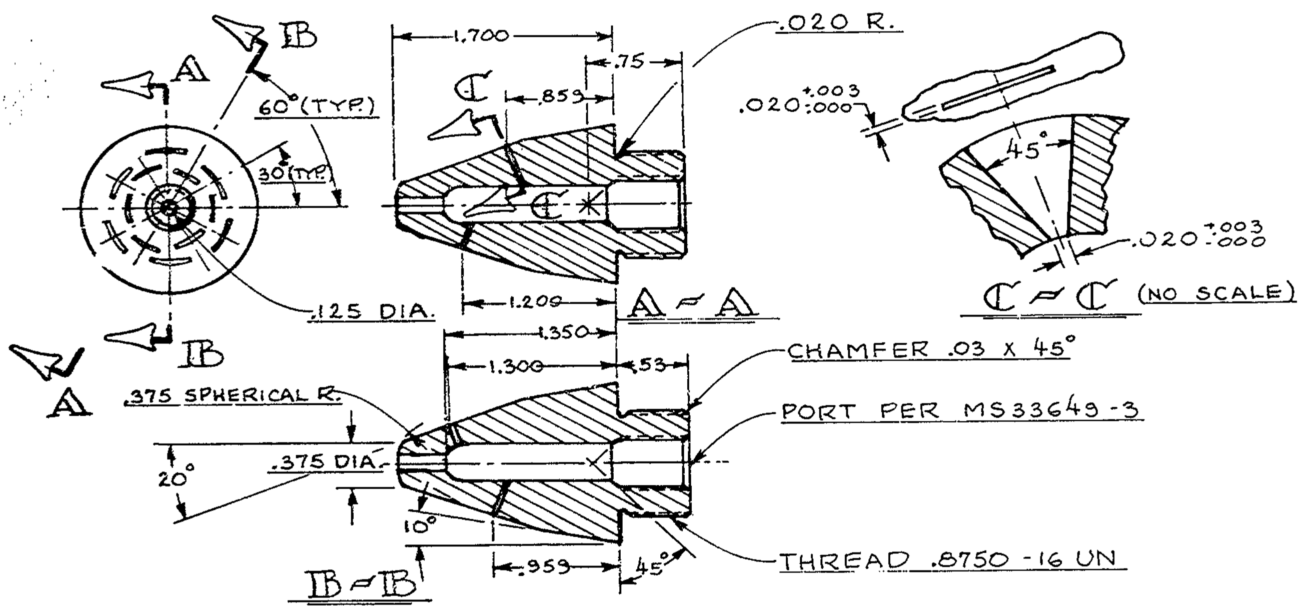

Figure 3-4. CONAF Discrete Hole Configuration 3

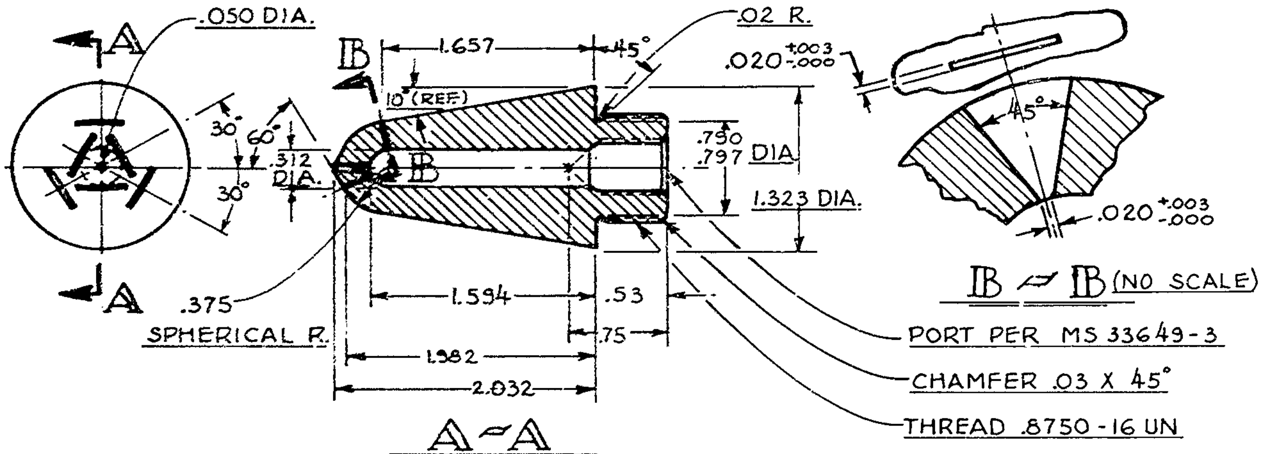

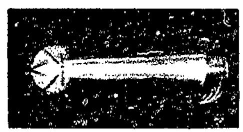

Figure 3-5. CONAP Discrete Hole Configuration 4

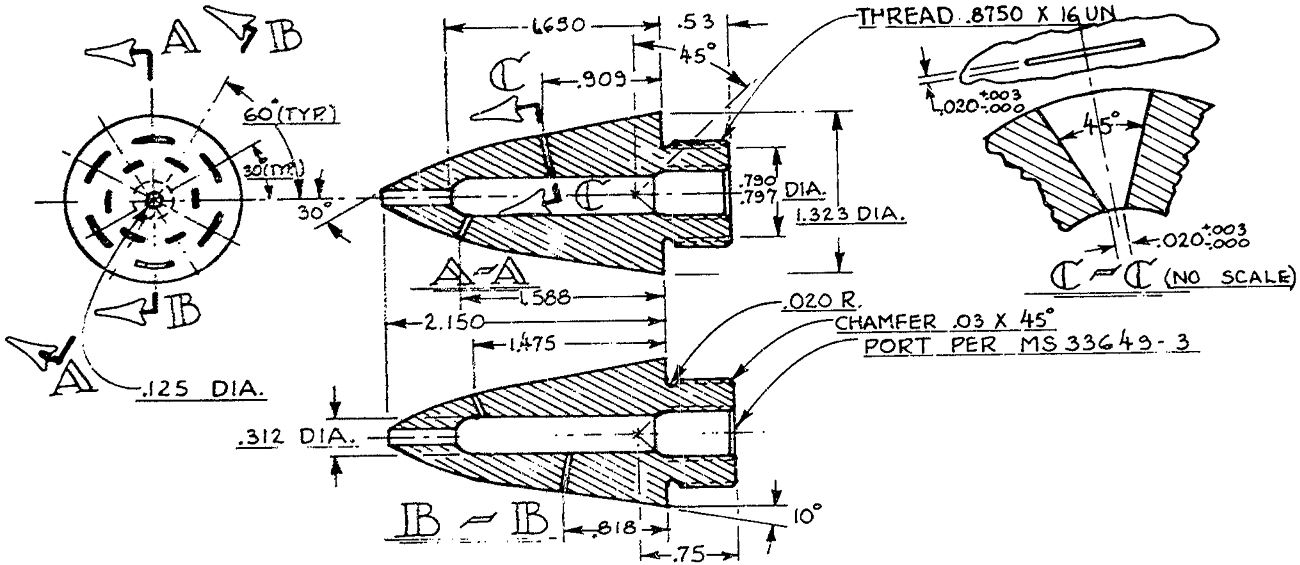

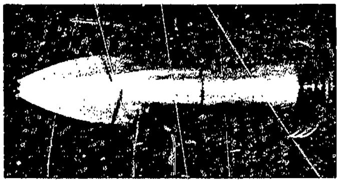

Figure 3–6. CONAP Discrete Hole Configuration 5

CONFIGURATION NUMBER	DESCRIPTION	ZERO-DEGREE ANGLE-OF-ATTACK	10-DEGREE ANGLE-OF-ATTACK
1	SPHERE-CONE WITH 1/8-INCH CENTERLINE HOLE		
2	SPHERE-CONE-CONE WITH 1/8-INCH CENTERLINE HOLE		
3	SPHERE-CONE-CONE WITH 1/8-INCH CENTERLINE HOLE AND SIDESLOTS		
4	60-DEGREE BICONIC WITH 50-MIL CENTERLINE HOLE AND SLOTS	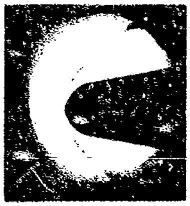	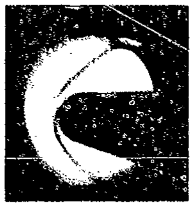
5	30-DEGREE OGIVE WITH 1/8-INCH CENTERLINE HOLE AND SIDE SLOTS		

Figure 3-7. Flow Visualization of CONAP Discrete Hole Matrices

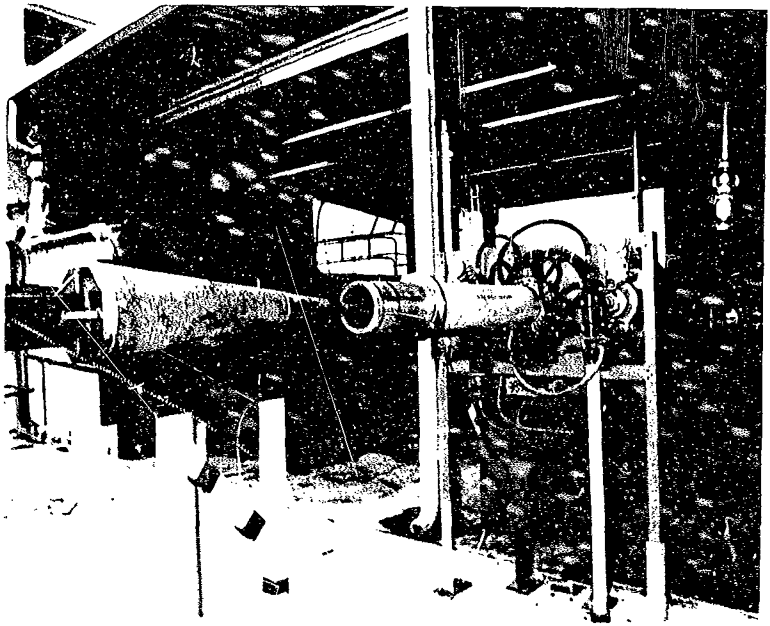

Figure 3-8. Model in Ramburner Test Setup

TABLE 3-I

Ramburner Test Conditions

$T_{stagnation}$	=	3100°R
$P_{stagnation}$	=	86 psia
M_w	=	0.7 lb/in^2 - s
D_{exit}	=	5 inches
γ	=	1.24
Model Material	=	Aluminum

TABLE 3-II

Test Results of Model No. 1

Sphere-Cone with 1/8-inch Centerline Hole

RUNs	Flow rate to Model lb/s	Test Time (Seconds)
1	0.397	10
2	0.195	10
3	0.129	10
4	0.068	10
5	0.051	10
6	0.034	10
7	0.026	10 Failed

TABLE 3-III

Test Results of Model No. 2

Sphere-Cone-Cone with 1/8-inch Centerline Hole		
Runs	Flow rate to Model lb/s	Test Time (Seconds)
1	0.069	10
2	0.0468	10
3	0.0348	10
4	0.0234	10 Model Failed

TABLE 3-IV

Test Results of Model No. 3

Sphere-Cone-Cone with 1/8-inch Centerline Hole and Sideslots		
Runs	Flow rate to Model lb/s	Test Time (Seconds)
1	0.097	10
2	0.065	10
3	0.0485	10
4	0.032	10
5	0.024	10 Survived with Onset of melt

TABLE 3-V

Test Results of Model No. 4

60-Degree Biconic with 60-mil Centerline Hole and Slots		
Runs	Flow rate to Model lb/s	Test Time (Seconds)
1	0.144	10 Melt around slots

TABLE 3-VI

Test Results of Model No. 5

60-Degree Ogive with 1/8-inch Centerline Hole and Side Slots		
Runs	Flow Rate to Model lb/s	Test Time (Seconds)
1	0.065	10
2	0.045	10
3	0.032	10
4	0.024	10
5	0.016	6 Failed at 6 seconds

TABLE 3-VII

Summary Results of Configuration Study

Model Description	Lowest Flow Rate at Which Model Survied in 10 Seconds	Flow Rate at Which Failed in 10 Seconds or Less
Sphere Cone	0.034 lb/s	0.026 lb/s
Sphere-Cone-Cone	0.0348	0.0234
Sphere-Cone-Cone with slots	0.024	-
60-degree biconic with slots	0.144	-
30-degree Ogive with slots	0.024	0.016

4.0 CONCLUSIONS AND RECOMMENDATIONS

During this study, three-dimensional nosetips were tested at both the 50 MW Plasma Arc Facility and the Martin Marietta Ramburner Facility. The testing conducted in the 50 MW facility compared and evaluated the performance of porous nosetip designs in a three-dimensional environment. The results of this test series in an environment which was more severe than expected, showed that: 1) two porous tungsten models performed well for the total test time of 4 seconds, 2) one model performed well for 1.2 seconds, but subsequently broke at the neck, and 3) one model failed at 0.3 sec, and the remaining two models did not receive sufficient coolant because of expulsion system venting. Of the five porous tungsten models tested, three porous models cracked longitudinally along the sidewall, and one broke at the neck during the tests. Only one of the models had no apparent cracking. Based upon this performance, it can be concluded that the CONAP porous tungsten matrix concept using a reactive gas operates successfully. The matrix material, however, requires considerable development to quality as a flight system nosetip candidate.

In addition to improvements in material strengths, improvements in the predictability of porous matrix flow characteristics will be required. It was found that, during the test series where flow modifications to the nosetips were to be evaluated, the flow tailoring efforts via material variations such as blind holes and vapor deposition were over-shadowed by the model-to-model variation in flow properties due to variations in the matrix. This suggests that the approach to fabricate nosetips from tungsten-copper stock does not yield sufficient control of the end item product. To specify, a priori, porous nosetip performance requirements, material fabrication methods must control porosity and flow properties, and must identify process variables. The continuation of the CONAP porous tungsten approach calls for a strong materials effort especially in the basic fabrication of the matrix where the original tungsten powders can be blended and sintered under defined conditions. This type of fabrication process control would be the next logical step in the development of the CONAP porous tungsten matrix concept.

The testing conducted in the Ramburner Facility evaluated the external configuration of the CONAP concept using the discrete hole matrix. The significant result of this evaluation was that a departure from the ordinary sphere-cone configuration was advantageous in terms of minimizing flow requirements. Two concepts in particular required less coolant than others considered: 1) the 30-degree ogive configuration with side slots and 2) the sphere-cone-cone configuration with sideslots. The next logical step in assessing these concepts is to verify these results at other angles-of-attack.

Future work in the development of the CONAP concept should concentrate on the following:

1. Development of porous tungsten material.

2. Assessment of discrete hole concepts at angle-of-attack.

3. Testing of the discrete hole concept in a plasma arc facility.

4. Assuming that viability of both concepts is demonstrated, combined ablation-erosion testing followed by full scale ground tests in a rocket exhaust facility should be performed.

REFERENCES

1. Ossin, A., Cawthon, D. M. "Evaluation of the CONAP Concept for Advanced ABM Nosetips," AMMRC CTR 74-1, January 1974

2. Nardacci, J. L., et al. Final Technical Progress Report, "Reentry Systems Environmental Protection (RESEP)," SAMSO-TR-68-463, March 1969, Secret Report

3. "Aerotip - An Advanced Transpiration-Cooled, Reentry Vehicle Nosetip," Aerojet General, June 1969, Aerojet Proprietary

4. Legendre, P.J. et al. Minutes of the Nosetip Briefing held August 22, 1969, at Aerospace, TOR-0066 (55816-36)-2

5. Kinnaird, L. D. "Controlled Atmosphere Protected Surfaces for Advanced Interceptor Missiles," presented at the 2nd Aerospace Structures Design Conference, September 28 and 29, 1970

6. Active Nosetip Evaluation Study, SAMSO Technical Report SAMSO-TR-73-74, November 1972.

7. Kinnaird, L. D., Cawthon, D. M., and Joyner, C. B. "Active Oxidation Protection for ABM Control Surfaces," AIAA Paper 71-391, April 1971

8. Ossin, A., Gafford, G., "Rain/Ice Erosion Resistant Nosetip/Heat Shield Evaluation and Development, Vol. II Erosion Resistant GASJET Nosetip" DNA 3562F-2, 1 March 1975

9. Ossin, Archie "Refractory Air Vane and Refractory Material Research and Development Task I - Refractory Air Vane Leading Edge for an Advanced Interceptor," AMMRC CTR 74-35, April 1974, Secret

10. The Fifty Megawatt Facility, TM 71-17 FXE, October 1971, AFFDL, Wright Patterson Air Force Base, Ohio

11. Brown-Edwards, et. al. "The Internal Shroud Nozzle - A New Concept for Testing Large Reentry Nosetips," AFFDL TM 72-34 FXE, October 1972

12. Rieckmann, R.E. "CONAP - Structural Analysis Report," ANA 10800000-010 August 13, 1974, Martin Marietta Corporation

13. Ossin, A. "Aerodynamic Heating and Heatshield Design," Martin Marietta, OR 12029, August, 1972

14. Brown-Edwards, E. G., "Fluctuations in Heat FLUX as Observed in the Expanded Flow From the RENT Facility ARC Heater," AFFDL TR-73-102, November, 1973.

APPENDIX I

COOLANT EXPULSION SYSTEM

1. COOLANT EXPULSION SYSTEM DESCRIPTION AND OPERATION

The coolant expulsion system is designed to provide anhydrous ammonia to a transpiration cooled nosetip. It is expected to provide a flow rate of approximately 0.10 lb/s at a pressure of 5000 psig. Design of the system is based on the functional concept of a previous system but is designed for higher pressure operation and incorporates several safety features not present in the original system. One of these features is a remotely actuated pressurization valve and a nitrogen vent valve which makes it unnecessary to approach the system while the ammonia is under high pressure. A system of hand valves helps to assure that ammonia will not leak from the system, due to its natural room temperature vapor pressure of 140 psia, when the system is depressurized. The system is mounted horizontally on a hand truck making it mobile and permitting ready access to every component in the system.

A schematic diagram of the coolant expulsion system is shown in Figure I-1, and a photograph of the system is shown in Figure I-2. Liquid anhydrous ammonia, stored in a high pressure accumulator, is pressurized with gaseous nitrogen to force the ammonia through the porous nosetip.

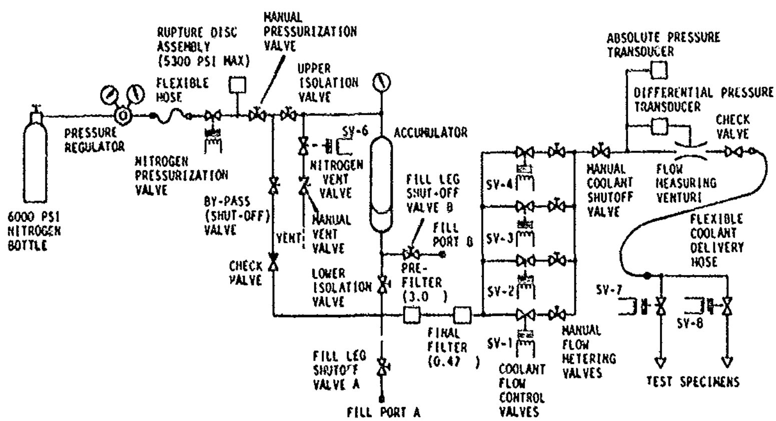

Figure I-1. Coolant Expulsion System Schematic

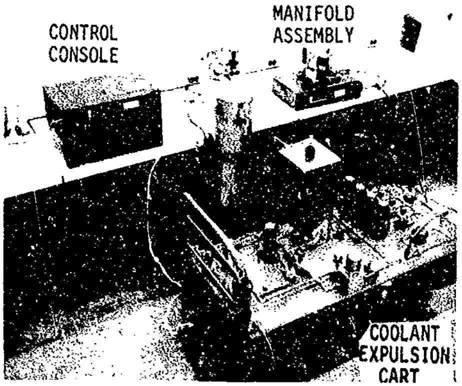

Figure I-2. CONAP Coolant Expulsion System

Gaseous nigrogen is supplied from a 6000 psi cylinder. A pressure regulator assures constant pressure while the coolant is being expelled from the system. Two pressurization valves, a hand shutoff and a solenoid valve, are employed to ensure that the ammonia will not be pressurized inadvertently, and both valves must be open to pressurize the system. The hand shutoff valve is opened during preparations for a test run. The solenoid valve is opened immediately prior to the start of a test run by an electrical signal from a remotely located control panel. A rupture disc assembly is located between the two pressurization valves. The rupture discs were selected to fail at 5300 psig.

Two vent valves (hand shutoff and solenoid) are included in the system to allow rapid dumping of system pressure. Both valves must be opened to allow the nitrogen pressure to vent. The hand shutoff valve will be opened during preparation for a test run. The solenoid valve will be opened at the end of a test run prior to approaching the system. It may also be opened during a test run in the event of an emergency. The solenoid valve is opened by an electrical signal from the remotely located control panel.

A bypass leg and bypass valve are provided to allow the system to be used to supply pressure regulated, flow rate controlled gaseous nitrogen as a coolant. The valve is also used in purging and filling operations. Normally it is closed during a test run. A check valve prevents ammonia from backing through the bypass leg where it might enter the upper part of the accumulator.

Hand shutoff valves are provided both upstream of the accumulator in the pressurization line and downstream of the accumulator in the ammonia line, to serve as isolation valves. These valves are necessary during fill and purge operations. Both of these valves are opened during preparations for a test run.

Pressurization of the liquid ammonia is provided by a hydropenumatic accumulator. The bladder type accumulator is filled to its rated capacity (2 1/2 gallons) with liquid anhydrous ammonia in the region external to the bladder. When the bladder is pressurized by opening both pressurization valves, the nitrogen pressure is transmitted to the ammonia.

Two fill legs and two fill leg shutoff valves are provided. These may be used in a variety of ways during fill and purge operations. Both valves are closed during preparation for a test run.

The anhydrous ammonia must pass through two filters prior to entering the flow control network. These filters assure that particulate matter will not interfere with closing of the flow control solenoid valves or cause clogging of the pores in the porous nosetip model. The prefilter uses a sintered stainless steel filter element designed to hold back particles larger than 3 microns. The final filter uses a replaceable paper element to hold back particles between 0.47 and 3 microns.

The flow control network consists of four parallel branches each of which includes a hand metering valve and a solenoid valve. The metering valves can be preset to pass a selected flow rate at a given coolant pressure. The solenoid valves can be separately actuated from the remotely located control panel to provide flow through one, two, three, or four branches simultaneously.

A hand shutoff valve downstream of the flow control network provides backup for the four solenoid valves to prevent leakage of ammonia in the event one or more of the solenoid valves should leak. This manual valve is left open during preparations for a test run.

Flow measurement is achieved with a venturi and a set of pressure transducers. The venturi is designed to provide a differential pressure of 500 psi at the design maximum flow rate. The differential pressure transducer is designed to provide a signal over the range from 0 to 500 psia and will withstand a differential pressure of 1000 psi. A check valve, immediately downstream of the venturi, will prevent damage to the venturi in the event of a system rupture upstream of the venturi. Without the check valve, such a failure would cause internal parts of the venturi to shear a snap ring and force the internal parts of the venturi upstream into the system.

The liquid ammonia flows through a flexible hose into a manifold which branches to two solenoid valves. These valves can be opened sequentially during a test run to allow coolant to flow through two test models in sequence.

2. PROCEDURE FOR FILLING THE ACCUMULATOR WITH AMMONIA

The system is prepared for charging by attaching a vacuum pump and pulling a vacuum on the part of the system normally filled with ammonia. The bladder is inflated to a few psi to expel all the gas in the accumulator external to the bladder. An ammonia cylinder is attached by a flexible harness to fill port B (see Figure I-1). The fill harness includes a bleed line to allow the harness to be filled with ammonia prior to admitting ammonia to the system. Nitrogen pressure in the bladder is decreased as necessary to admit ammonia into the accumulator. Initially, part of the ammonia will vaporize. In due time, the vapor will condense and liquid ammonia will continue to flow into the accumulator. When the beam balances on the platform scales, indicating that 14 pounds (2 1/2 gallons) of ammonia has flowed into the system, the fill leg valve is closed, and the cylinder valve is closed. The bleed valve is opened on the fill harness to allow the ammonia in the line to boil off.

To avoid dumping ammonia into the air during the bleed operations, the fill harness is attached to a suction tee to which a garden hose carries tap water. The mixed ammonia and water coming out of the suction tee is carried to a suitable drain or open area by a garden hose.

Since there are no means to gage the quantity of ammonia remaining in the accumulator following a test run, it is necessary to dump the remaining ammonia and recharge the system between test runs. Dumping employs the suction tee and tap water arrangement used for bleed operations. It is not necessary to use a vacuum pump prior to recharging when the system already contains ammonia.

3. INTERFACING HARDWARE

During the 50 MW testing, plumbing connections were required from the coolant manifold to the coolant conduit in both stings on which a test model was mounted. The plumbing on the exit sides of the two manifold valves were 3/8-inch AN male fittings. The fitting on the coolant conduits provided a 3/8-inch AN male fitting.

Interconnections were made with 3/8-inch, 0.049-inch wall stainless tubing and Parker 37-degrees flare fittings or other fittings suitable for pressures to 4000 psi. Interconnections can also be made with suitable high pressure flexible hose. If flexible hoses are employed, care should be taken to ensure that the lining is compatible with liquid anhydrous ammonia.

4. REMOTE OPERATION OF EXPULSION SYSTEM

A remotely located control system permits both automatic and manual control of the coolant expulsion system. The manual shutoff valves and metering valves must be preset prior to a test run to enable the remote control system to properly perform its functions. A schematic diagram of the remotely located control system is shown in Figure I-3. The electrical equipment located at the coolant expulsion system is shown schematically in Figure I-4. The control panel is shown in Figure I-5.

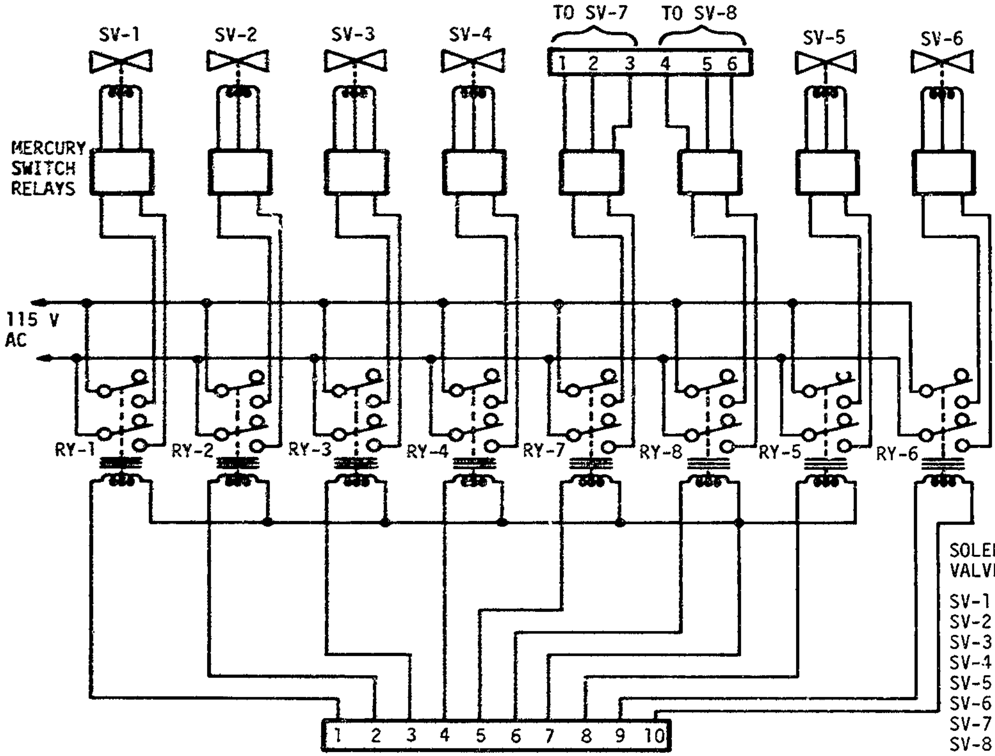

SOLENOID VALVE NO.	FUNCTION
SV-1	FLOW
SV-2	CONTROL
SV-3	NETWORK
SV-4	↓
SV-5	PRESSURIZATION
SV-6	NITROGEN VENT
SV-7	SPECIMEN-SELECTOR
SV-8	SPECIMEN SELECTOR

Figure I-3. Control System

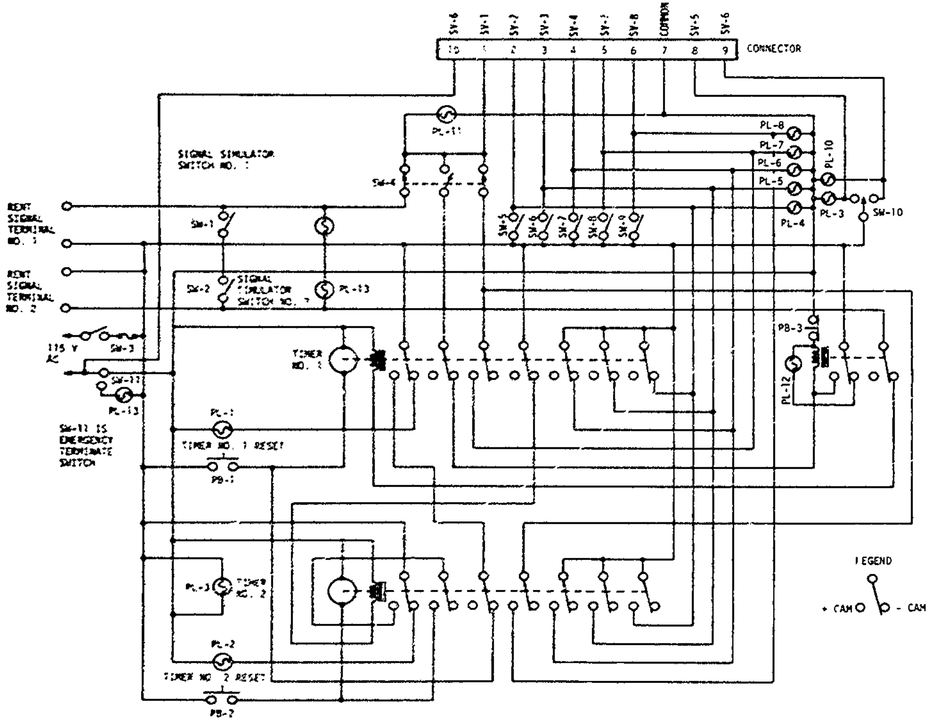

SWITCH NO.	DESCRIPTION
1	SPST 10 AVP
2	SPST
3	SPST
4	SPDT
5	SPST
6	SPST
7	SPST
8	SPST
9	SPST
10	SPDT 10 AMP NEUTRAL POSITION (SELECTS PRESSURE OR VENT MODES)
11	SPDT

PUSH BUTTON NO.	DESCRIPTION
1	N.O.
2	N.O.
3	N.C. (BREAKS LATCH CIRCUIT IN RY-9 TO ALLOW REPEAT CYCLE)

PILOT LAMP NO.	INDICATION
1	TIMER NO. 1 IS RESET
2	TIMER NO. 2 IS RESET
3	AC POWER IS ON
4	SV-2 IS OPENED
5	SV-3 IS OPENED
6	SV-4 IS OPENED
7	SV-7 IS OPENED
8	SV-8 IS OPENED
9	SV-5 IS OPENED
10	SV-6 IS OPENED
,	SV-1 IS OPENED
12	RY-9 IS OPENED
13	EMERGENCY TERMINATE ON

Figure I-4. Electrical Equipment

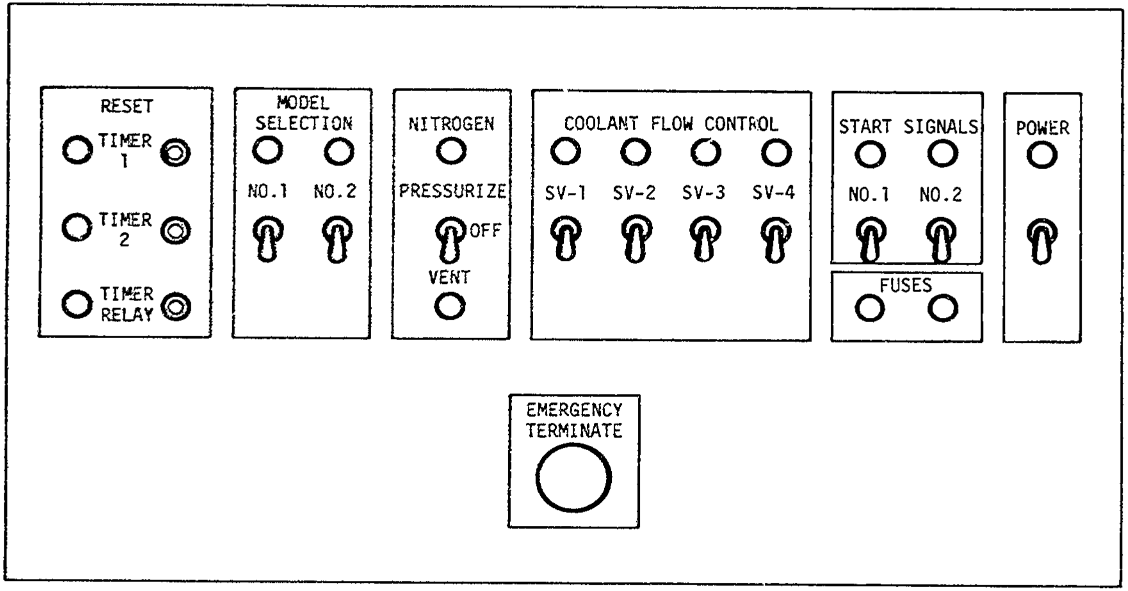

Figure I-5. Remotely Located Control Panel

The automatic features of the control system are achieved with two cam type timers and a relay. Prior to a test run, the power is turned on, the nitrogen pressurization switch is turned on, and each of the three reset buttons is pushed until the corresponding green light comes on. Simultaneous with the starting of the plasma jet, a switch is automatically closed (Signal 1) which opens one of the solenoid valves in the flow control network and the manifold valve admitting coolant to specimen 1. Simultaneous with the start of the carriage, a second switch is automatically closed which starts timer 1. Timer 1 immediately actuates switches which open the remaining three valves in the flow control network so that when specimen 1 reaches the jet, the coolant flow rate is at the maximum level. At preset time intervals these same three valves close sequentially causing the coolant flow rate through the test specimen to decrease in steps. About the time specimen 1 leaves the jet, timer 2 is actuated and immediately all of the flow control valves are opened. At this point, timer 1 is stopped. When specimen 2 enteres the jet, the flow control valves repeat their routine, when timer 2 stops, signals 1 and 2 are removed, and nitrogen pressure is dumped by briefly actuating the vent valve switch and observing the coolant absolute pressure monitor. The reset buttons are pushed until each green light comes on. Power is then shut off. Should an emergency occur during a run, an abort switch can be actuated which removes power from all the valves except the nitrogen vent valve.

APPENDIX II

FACILITIES

1. AFFDL 50 MW PLASMA ARC FACILITIES*

The Air Force Flight Dynamics Laboratory's 50 MW Plasma Arc Facility consists of the Reentry Nosetip (RENT) test leg and the Hypersonic Test Leg (HTL). Pitot pressures up to 100 atm and heating rates of 18,000 BTU/ft^2-s to a 0.25-inch nose radius tip can be obtained with the RENT test leg. This leg is used basically for nosetip testing. The HTL test leg can simulate heating rates corresponding to Mach numbers from 8 to 13 with 30-minute run times and is used primarily to test and evaluate aerothermal structures and thermal protection systems associated with reentry heating. The HTL test leg can accept models up to 6 feet in length.

Both legs of the plasma arc share a common air supply, electrical power supply, cooling water system, and data acquisition system.

a. Arc Heaters

The key components of the facility are the high pressure, high voltage arc heaters. The N-4 heaters presently used can heat up to 7 lbm/s of air to enthalpies of 2000 to 6200 BTU/lbm at pressures up to 125 atm. The air is heated with a direct current arc, vortex stabilized along the axis of two water cooled tubular copper electrodes in coaxial tandem arrangement. The arc attachment points are stabilized axially and rotated around the inside walls of the electrodes by the combined action of electromagnetic coils and the air vortex.

By varying the direction and velocity of the air injected into the arc heater, the energy distribution across the test section can be varied from flat to peaked, with centerline enthalpy values nearly twice those found in the surrounding flow. A flat enthalpy distribution is usually used in the Hypersonic Test Leg and peaked in the RENT leg. Varying the internal airflow and facility power conditions produces enthalpies from 1,200 BTU/lbm to 6,200 BTU/lbm in the center of the test jet. Contamination of the air delivered to the test section, consisting principally of copper compounds from the electrodes, is less than 0.1 percent by weight and is generally confined to the flow field perimeter.

---

*AFFDL 50 MW Plasma Arc Facility description consists of excerpts from Reference 10.

b. Data Acquisition and Recording

The two test legs share a common computer-based data acquisition system which is built around an AMBILOG 200 hybrid computer. In the normal data recording mode, 262 channels of data can be sampled each second, converted to the proper engineering units, and recorded on magnetic tape. Not all of the 262 data channels are available for model instrumentation. The number available for model instrumentation is dependent on the signal conditioning equipment used and on the overall requirements of the test program. On-line computation of derived data is performed using multi-sample averages of the raw data, and any four items of data can be presented with 1 second update on a "nixie" tube display in the control room for monitoring the test. In the high speed mode, used for RENT leg model data acquisition, up to 6 channels per model strut position can be sampled and recorded at 1 ms intervals. Additional channels of high speed data can be recorded on oscillographs. After a test run the basic and computed data are retrieved from the magnetic tape and printed at 1000 lines per minute.

c. RENT Test Leg

The RENT test leg produces a high enthalphy, high pressure airstream ideally suited to the study of ablation phenomena. Other high pressure, high heating rate tests dealing with transpiration cooling and internally water cooled leading edges can also be accomplished.

A schematic of the major system components is shown in Figures II-1 and II-2. The use of an atmospheric-pressure free-jet test section is possible because the flow from the RENT nozzles is underexpanded to produce high pitot pressures. Pitot pressures up to 100 atm and stagnation point heat fluxes of 18,000 BTU/ft^2-s have been measured on 0.25-inch radius hemispherical nosetip models. These values of pressure and heating rate correspond to a total enthalpy of 6,200 BTU/lbm.

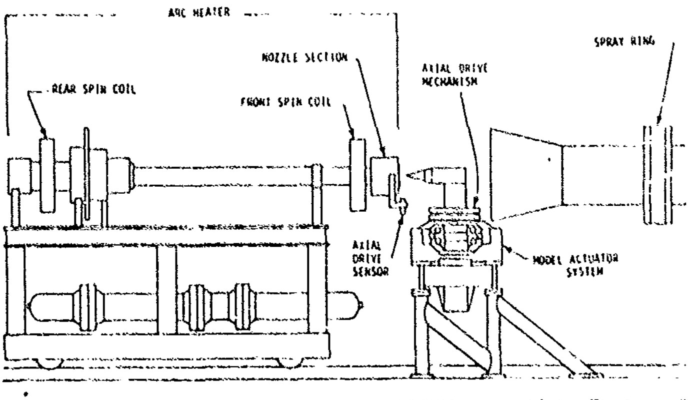

Figure II-1. RENT Test Leg Schematic

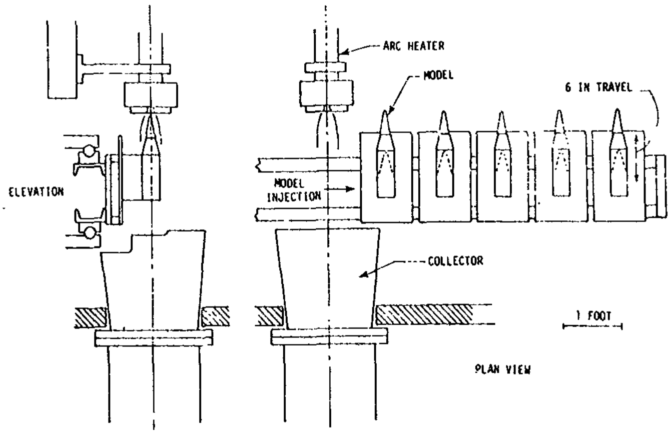

Figure II-2. RENT Test Section and Model Support

1) Model Support System

A linear motion model carriage is used for insertion of the models or probes into the test flow. The carriage has five model struts laterally spaced 1 foot apart. All model struts and associated hardware are water cooled. Water cooling can also be provided for models as required.

The model carriage operation can be programmed so that each strut has one of two types of exposure to the test flow. A model or probe can be held on the flow centerline for a specified duration or swept across the test flow at a specified velocity which may range from 1 to 100 in/s. Each of the five struts has an axial drive system that can be servo-controlled to keep the nosetip of an ablating model at a given axial station or be remotely adjusted to any set point within its 6 inch range of travel.

The five struts are designed to accept a standard hemisphere-cone model of 2-inch base diameter and a 10-degree cone half-angle. However, with the approval of the AFFDL project engineer, other shapes and sizes can be adapted to the facility.

2) Data Acquisition and Recording

As mentioned earlier, the key facility parameters can be continuously monitored from displays in the control room. In addition, test point data taken at selected intervals are recorded on magnetic tape by the computer and printed out on request. In its high-speed mode, the computer system can sample and record each of six channels at 1-ms intervals from each strut. Also, two CEC Visicorders are available for strip chart displays of about 12 channels per strut, depending on the type of data being recorded.

In addition to the above data acquisition systems, two Photosonic and one Hycam motion picture cameras are available. The general characteristics of these cameras are listed in Table II-1. The two Photosonic cameras receive a 1 kHz signal from the computer from which a digital time is generated and printed in a coded decimal form on each film frame. The 1 kHz signal is also recorded on the Visicorders, enabling all of the analog and digital data to be correlated in time.

TABLE II-I

Available RENT Leg Photographic Equipment

Camera	Negative Size	Remarks
Photosonic	16mm	Use: RENT leg High speed computer time displayed on each film frame. Frame rate: 24 to 1,000/s Magazine capacity: 400 ft or 1200 ft Normally available: 2
Mitchell	16mm	Use: RENT leg 1 kHz timing marks available Frame rate: 24 to 400/s Magazine capacity: 400 ft Normally available: 2
Hycam	16mm	Use: RENT leg 1 kHz timing marks available Frame rate: 8 to 128/s Magazine capacity: 400 ft Normally available: 1
Mitchell	16mm	Use: RENT leg and Hypersonic leg Frame rate: 8 to 128/s Magazine capacity: 400 ft Normally available: 1

3) Nozzles

Three types of nozzles are presently available for the RENT arc heater: 1) contoured nozzles for parallel flow, 2) conical nozzles, and 3) flared nozzles. The nozzles are made of zirconium copper alloy and are of thin wall design with high pressure and high velocity backside water cooling. They are suitable for arc heater operation up to 1800 psi chamber pressure.

The shrouded nozzles are designed to surround the hot core with a large cold-flow pressure field which will permit thermostructural tests of larger test articles and of bodies at different angles-of-attack. The cold shroud flow is added through an annular slot upstream of the nozzle throat. These nozzles require cold mass flow rates 5 to 15 times the heated mass flow.

2. VACUUM FURNACE

A vacuum furnace was employed to boil off the copper from the porous tungsten specimens. This furnace (shown in Figure II-3) consists of a water cooled stainless steel tank with a viewing port and a gas tight gland through which a water cooled RF coil is passed. A high capacity diffusion vacuum pump is also attached through a series of valves and a liquid nitrogen cold trap to the stainless steel tank. A 5 kW RF generator is connected to the RF coil and provides the heat to boil off the copper. Boiling off the copper in the prescence of a vacuum is necessary both to prevent tungsten oxidation and to achieve copper boiling at relatively low temperatures (copper boils at 2200°F at a pressure of 2.5 x 10^{-3} mm of Hg). This facility was capable of achieving both these conditions.

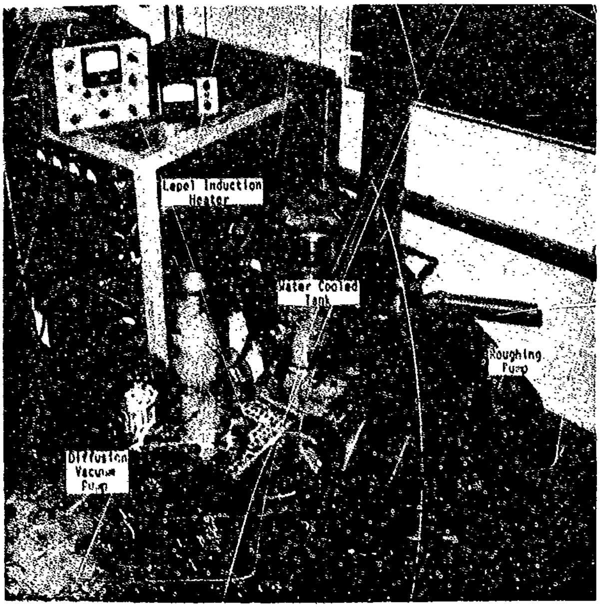

Figure II-3. Vacuum Evaporation Equipment for Copper Removal

3. RAMBURNER TEST FACILITY

The Martin Marietta Ramburner Test Facility delivers high temperature vitiated air to the test article from a blowdown system. The ramjet combustor burns over a pressure range from 30 to 300 psia and has a variable controlled combustion temperature from 2500°R to 4500°R. An inlet temperature is controlled by an O_2-H_2 preheat system. The combuster characteristically burns JP-4 fuel, although other fuels have been used. A summary of the available test conditions is given in Table II-II.

The facility is shown in Figure II-4 and a system schematic is shown in Figure II-5. Gas flow is controlled through automatic sequencing equipment.

TABLE II-II

Subscale Ramburner Facility Operational Capability

Available Air (lb)	Air Flow (lb/s)	Fuel Flow (lb/s)	Air Temperature (°R)/O_2H_2)	Air Pressure (psia)	Combustor Gas Temperature (°R)	Combustor Pressure (psia)
300	1 to 25	0.05 to 2.0	520 to 2000 for 10 min+	30 to 350	2500 to 4500	30 to 300

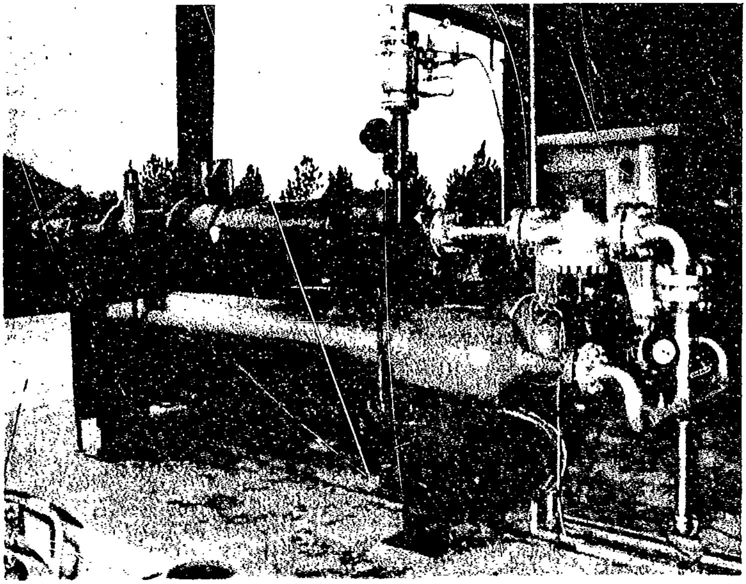

Figure II-4. Subscale Ramburner Test Facility

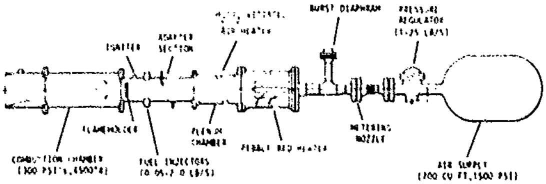

Figure II-5. Subscale Ramburner Test Facility Schematic

APPENDIX III

SPRINT Specification 11181124

REVISIONS

MF	SYM	SHEET	DESCRIPTION	DATE	APPROVED
			ALL PREVIOUS REVISIONS ARE RECORDED ON MICROFILM. LAST INCORPORATED NOR 4		
4-✓ 6/2/70	E		INC NOR 5, X38662 ADDED PARA 4.3.2 – 4.3.7 AND 5.3. RELEASED TO PRODUCTION. J.A. Maulding 3-2-7- WAS 11181124X ECP 250009 APPROVED 06 JUNE 70	17 APR 70	R. E. Dunlap (R)
3/2✓	F		INC NOR 6, X51477, ECP251163R-C- 13 MAR 74	14 MAR 74	(R)

SOURCE CONTROL DRAWING

INTERPRET DRAWING IN ACCORDANCE WITH MIL-D-1000, FORM I, CATEGORY P

PREPARED BY:
MARTIN COMPANY
ORLANDO, FLORIDA
32805

SEE ENGINEERING RECORDS*

NEXT ASSEMBLY	USED ON
APPLICATION	

DO NOT APPLY PART NO.

PL	F DWG	REV LEVEL

~~PARTS LIST PL~~

ARMY PART NO. 11181124

CONTRACT NO. DA-30-069-AMC-333(Y)

MARTIN CO DIVISION OF MARTIN MARIETTA CORP
FOR BELL TELEPHONE LABORATORIES INCORPORATED

U S ARMY MATERIEL COMMAND
REDSTONE ARSENAL, ALABAMA

ORIG DWG DATE: 6 Jul 64	
DRAFTSMAN: G. Steiner	CHECKER: Loeffler
ENGR: J.P. Cooper	ENGR: F.J. Angiulli
ENGR:	APPROVED: H. Goplen

TUNGSTEN-COPPER BARS, PLATES AND RODS

APPROVED

BY ORDER OF C G AMC

C. L. Conklin

CODE IDENT NO.	SIZE	
17773	A	11181124
SCALE	UNIT WT	SHEET 1 OF 9

FORM 2105-A CASE NO. PROJECT

APPROVED

Form 2302

SHEET/REVISION INDEX

SHEET	REV.	SHEET	REV.	SHEET	REV.	SHEET	REV.	SHEET	REV.	SHEET	REV.	SHEET	REV.
1	F												
2	F												
3	F												
4	E												
5	E												
6	F												
6a	F												
7	E												
8	E												

CODE IDENT. NO.	SIZE	
17773	A	11181124
SCALE	REV. F	SHEET 2

Form 2013-A3

1. SCOPE

1.1 This specification covers one type of pressed and sintered porous tungsten, infiltrated with copper. This material is prepared by powder metallurgical techniques in the form of bars, rod or plate.

2. APPLICABLE DOCUMENTS

2.1 The following documents of the issue in effect on the date of invitation for bids or request for proposal, form a part of this specification to the extent specified herein.

SPECIFICATIONS

<u>Federal</u>

QQ-A-673	Anodes, Copper

<u>Military</u>

MIL-I-6866	Inspection, Penetrant, Method of

STANDARDS

<u>Federal</u>

FED-TEST-METHOD-STD-151	Metals, Test Methods

<u>Military</u>

MIL-STD-129	Marking for Shipment and Storage

(Copies of specifications, standards, drawings and publications required by supplier in connection with specific procurement functions should be obtained from the procuring activity or as directed by the contracting officer.)

2.2 <u>Other publications</u>.- The following documents form a part of this specification to the extent specified herein. Unless otherwise indicated, the issue in effect on date of invitation for bids or request for proposal shall apply:

<u>American Society for Testing and Materials</u>

ASTM-E-2	Standard Methods of Preparation of Micrographs of Metals and Alloys
ASTM-E-8	Methods of Tension Testing of Metalic Materials
~~ASTM-E-107~~	~~Standard Method of Chemical Analysis of Electronic Nickel~~

F

SIZE	CODE IDENT NO.	
A	17773	11181124
SCALE	REV F	SHEET 3

ASTM-E-112	Standard Methods for Estimating the Average Grain Size of Metals

(Application for copies of ASTM publications may be obtained from the American Society for Testing and Materials, 1916 Race Street, Philadelphia , Pennsylvania 19103.)

Society of Automotive Engineers

AMS 2630	Ultrasonic Inspection

(Application for copies of AMS publications may be obtained from the Society of Automotive Engineers Inc., Department 010, Two Pennsylvania Plaza, New York, New York, 10001.)

(Technical society and technical association specifications and standards are generally available for reference from libraries. They are also distributed among technical groups and using Federal agencies.)

3. REQUIREMENTS

3.1 Qualification.- The material furnished under this specification shall be a product which has been tested, and passed the qualification tests specified herein.

3.1.1 Requalification.- The supplier is advised that if the material formulation r construction has been changed since the receipt of qualification approval, samples hall be submitted for reapproval before supplying material to the requirements of this specification.

3.1.2 Source information.- Only the item(s) listed on this drawing and identified by the vendor's name(s), address(es), and part number(s) have been tested and approved by Safeguard System Command for use in the Safeguard System. A substitute item shall not be used without prior testing and approval by Safeguard System Command.

3.2 Material.- The material shall be supplied in the as sintered and infiltrated condition. It shall be a porous tungsten base of uniform particle size manufactured by powder metallurgical processes and infiltrated with copper. After sintering, the porous tungsten base shall be of uniform density (78 to 82% of theoretical). Not less than 95% of the pores shall be interconnecting. The infiltration efficiency shall be at least 90%.

3.2.1 Component proportions.-

Tungsten	78 to 82 volume % (89 to 91 weight %)
Copper	16 to 22 volume % (8 to 11 weight %)

3.3 Chemical composition of components.-

	Tungsten	Copper
Carbon	50 ppm maximum	QQ-A-673, Type II Requirements
Oxygen	100 ppm maximum	

SIZE	CODE IDENT NO	
A	17773	11181124
SCALE	REV E	SHEET 4

3.3 Chemical composition of components (continued).-

Tungsten	
Nitrogen	50 ppm maximum
Tungsten	99.93% minimum

3.4 Density and ultimate tensile strength.- The sintered and infiltrated material shall have the following properties at room temperature:

Density	16.8 to 17.3 gms/cc
Ultimate tensile strength	60,000 psi minimum

3.5 Microstructure and grain size.- The microstructure shall exhibit a uniform distribution of tungsten and copper. The grain size of the tungsten shall be 0.010 mm., maximum, when examined at 100 magnification. The size of the copper filled areas shall not exceed the tungsten grain size.

3.6 Defects.-

3.6.1 Surface defects.- No cracks or discontinuities are permissible as determined by penetrant inspection.

3.6.2 Internal defects.- The material shall be sound and free of internal defects.

3.7 Marking.- Each container for the materials covered by this specification shall be marked in a permanent manner with the following information:

a. This specification number and revision level

b. Supplier's name, address, and designation

c. Purchase order number.

3.8 Workmanship.- The material shall be uniform in texture, free from impurities and other defects that would prevent its use for the purpose intended, or that will adversely affect life, serviceability, or appearance.

4. QUALITY ASSURANCE PROVISIONS

4.1 Responsibility for inspection.- Unless otherwise specified in the contract or purchase order, the supplier is responsible for the performance of all inspection requirements as specified herein. Except as otherwise specified, the supplier may utilize his own facilities or any commercial laboratory acceptable to the procuring activity. The procuring activity reserves the right to perform any of the inspections set forth in the specification where such inspections are deemed necessary to assure supplies and services conform to the prescribed requirements.

4.2 Classification of tests.- Inspection and testing shall be classified as follows:

a. Qualification tests

b. Quality conformance tests

4.2.1 Qualification tests.- Qualification tests shall consist of tests for all requirements of this specification.

4.2.2 Quality conformance tests.- Quality conformance tests shall consist of tests for the following requirements for each lot.

Test or inspection	Requirement	Test method
Density	3.4	4.3.1
Visual	3.8	4.7

4.3 Test methods.-

4.3.1 Density.- The water displacement method of measuring density shall be used. For samples under 200 grams, a suspended pan balance with a sensitivity of 0.0005 grams is used. For samples between 200 and 2000 grams a suspended pan balance with a sensitivity of 0.01 grams is employed. Distilled water to which 5 drops per 1000 ml (of water) of an aerosol wetting agent has been added is used for immersion of the samples. The sample is suspended in the water by means of a fine wire of sufficient size to safely carry the load. Density is calculated by the usual formula:

$$D = \frac{\text{Weight in air (grams)}}{\text{Loss of weight in water (grams)*}}$$

*Values used in this formula must be corrected for the weight of the suspension wire.

4.3.2 Chemical composition of components.- The chemical composition of the copper shall be determined in accordance with Method 111.2 of FED-TEST-METHOD-STD-151. The oxygen and nitrogen content of the skeletal tungsten shall be determined in accordance with the procedure and equipment of LECO TC-30 Simultaneous Nitrogen-Oxygen Determinator, Laboratory Equipment Corporation, 300 Lakeview Avenue, St. Joseph, Michigan 49085, or equivalent. The carbon content of the skeletal tungsten shall be determined in accordance with the procedure and equipment of LECO Gasometric Carbon Analyzer, Laboratory Equipment Corporation, 300 Lakeview Avenue, St. Joseph, Michigan 49085, or equivalent. The tungsten content shall be determined in accordance with Method 111.2 or 112.2 of FED-TEST-METHOD-STD-151.

F

4.3.3 Ultimate tensile strength.- The ultimate tensile strength shall be determined in accordance with ASTM-E-8.

4.3.4 Microstructure.- The microstructure shall be determined in accordance with ASTM-E-2.

4.3.5 Grain size.- The grain size shall be determined in accordance with ASTM-E-112.

4.3.6 Surface defects.- Surface defects shall be determined in accordance with MIL-I-6866, Type I, penetrant inspection.

4.3.7 Internal defects.- Internal defects shall be determined in accordance with AMS-2630, ultrasonic inspection.

4.4 Test conditions.- Unless otherwise specified in the test procedures, tests shall be conducted at a temperature of 77 ±10° F and the relative humidity shall be 30 to 70 percent.

4.5 Examination of product.- All samples of material shall be examined carefully to determine conformance to this specification with regard to requirements not covered by specific test methods.

4.6 Examination of preparation for delivery.- Preparation for delivery of materials ready for shipment shall be examined to determine conformity to the requirements of Section 5.

4.7 Visual inspection.- All samples of material shall be examined carefully to determine conformance to the requirements specified in 3.8.
Unless otherwise specified, all visual examinations shall be conducted with an unaided eye, except for normal corrected vision.

4.8 Rejection.- Failure to meet any requirements of this specification shall be cause for rejection of the entire lot.

4.9 Vendor report.- Vendor shall submit with each shipment a certified report of compliance to the requirements of this specification.

5. PREPARATION FOR DELIVERY

5.1 Packaging.- The materials are normally supplied in crates, boxes or cartons.

5.2 Packing.- The material shall be prepared for shipment in accordance with commercial practice to insure carrier acceptance and safe transportation at the lowest rate of delivery and shall meet, as a minimum, the requirements of carrier rules and regulations applicable to the mode of transportation.

5.3 Marking of shipments.- Each shipping container shall be marked in a permanent manner in accordance with MIL-STD-129 where applicable, with the following information:

a. This specification number and revision level, and item classification

b. Supplier's name, address, and designation

c. Date of shipment

d. Purchase order number

e. Lot number

6. NOTES

6.1 Intended use - Parts fabricated from this material are intended for use in extreme high temperature and oxidizing environments.

6.2 Definitions.-

6.2.1 Lot.- A lot shall consist of all material delivered for acceptance at one time which has been fabricated from one batch of raw materials.

6.3 Ordering data.- Procurement documents shall include the following:

(a) Title, number, and revision level of this specification

(b) Supplier's item identification number, name, and address

(c) Quantity of material required

6.4 Approved source(s) of supply.-

Teledyne Wah Chang Albany
Albany, Oregon 97321

Sylvania Electric Products Co.
Towanda, Pennsylvania 18848

SUPERSEDING
Fed. Spec. QQ-A-673
June 2, 1958

FEDERAL SPECIFICATION

ANODES, COPPER

This specification was approved by the Commissioner, Federal Supply Service, General Services Administration, for the use of all Federal agencies.

1. SCOPE AND CLASSIFICATION

1.1 **Scope.** This specification covers copper anodes for use in electroplating baths.

1.1.1 *Federal specification coverage.* Federal specifications do not include all varieties of the commodity as indicated by the title of the specification, or which are commercially available, but are intended to cover only those generally used by the Federal Government.

1.2 Classification.

1.2.1 *Types.* Copper anodes shall be of the following types, as specified (see 6.2):

Type I.—Non-deoxidized.

Type II.—Oxygen free.

Type III.—Deoxidized, phosphorus bearing.

2. APPLICABLE SPECIFICATIONS AND STANDARDS

2.1 The following specifications and standards, of the issues in effect on date of invitation for bids or request for proposal, form a part of this specification:

Federal Specifications:

PPP-B-585—Boxes, Wood, Wirebound.

PPP-B-601—Boxes, Wood, Cleated-Plywood.

PPP-B-621—Boxes, Wood, Nailed and Lock-Corner.

Federal Standards:

Fed. Std. No. 102—Preservation, Packaging, and Packing Levels.

Fed. Std. No. 123—Marking for Domestic Shipment (Civil Agencies).

Fed. Test Method Std. No. 151—Metals; Test Methods.

(Activities outside the Federal Government may obtain copies of Federal Specifications, Standards, and Handbooks as outlined under General Information in the Index of Federal Specifications, Standards, and Handbooks and at the prices indicated in the Index. The Index, which includes cumulative monthly supplements as issued, is for sale on a subscription basis by the Superintendent of Documents, U. S. Government Printing Office, Washington, D. C. 20402.

(Single copies of this specification and other product specifications required by activities outside the Federal Government for bidding purposes are available without charge at the General Services Administration Regional Offices in Boston, New York, Washington, D. C., Atlanta, Chicago, Kansas City, Mo., Dallas, Denver, San Francisco, and Auburn, Wash.

(Federal Government activities may obtain copies of Federal Specifications, Standards, and Handbooks and the Index of Federal Specifications, Standards, and Handbooks from established distribution points in their agencies.)

Military Standards:

MIL-STD-105 — Sampling Procedures and Tables for Inspection by Attributes.

MIL-STD-129—Marking for Shipment and Storage.

(Copies of Military specifications and standards required by suppliers in connection with special procurement functions should be obtained from the procuring activity or as directed by the contracting officer.)

3. REQUIREMENTS

3.1 Materials. Anodes shall be of solid copper. They shall be either cast, forged, rolled to size, or cut to size from electrolytic cathodes, castings, or rolled plates.

3.2 Size, shape, and method of suspension. The size, shape and method of suspension (when applicable) of the anodes shall be as specified (see 6.2).

3.2.1 Ball anodes shall have a diameter of approximately 2 inches and weigh not less than 1-1/4 pounds. Sheared bar and shapes with one or both ends hemispherical are acceptable provided that the overall length does not exceed four inches. For type II copper anodes only, cut bars with a maximum length of four inches and a maximum diameter of two inches will be acceptable.

TABLE I.—*Chemical composition*[2]

	I	II	III
Copper, percent[1]	99.90 min.	99.95 min.	99.90 min.
Iron, percent	0.003 max.	0.002 max.	0.003 max.
Sulfur, percent	0.003 max.	0.003 max.	0.003 max.
Lead, percent	0.003 max.	0.002 max.	0.002 max.
Antimony, percent	0.002 max.	0.002 max.	0.002 max.
Nickel, percent	0.003 max.	0.002 max.	0.002 max.
Total metallic impurities, percent	0.01 max.	0.01 max.	0.01 max.
Oxygen, percent	0.045 max.	—	—
Phosphorus, percent	—	0.001 max.	0.015 to 0.040

[1] Silver is counted as copper.

[2] Analysis shall be made only for the elements specifically mentioned in the above table. If, however, the presence of other elements is indicated in the course of routine analysis, further analysis shall be made to determine that these other elements are not present in excess of the limits specified.

3.3 Chemical composition. Unless otherwise specified in the contract or order (see 6.2), the composition of the copper anodes shall meet the requirements shown in table I.

3.3.1 An analysis for each lot of anodes shall be furnished by the contractor showing the percent of the elements designated in table I.

3.3.1 An analysis for each lot of anodes shall be furnished by the contractor showing the percent of the elements designated in table I.

3.4 Cuprous oxide. Types II and III anodes shall be free from cuprous oxide when tested in accordance with the microscopic test as specified in 4.5.2.

3.5 Identification. Each anode, except ball anodes, shall be permanently identified with the following information:

(a) "ANODE, COPPER"
(b) Specification number
(c) Type classification

3.5.1 *Ball anodes.* Each ball anode shall be permanently marked with the word "copper" or the symbol "Cu," either as the result of casting or otherwise imprinting the selected identifying mark.

3.6 Workmanship. Anodes shall be clean and substantially free from cracks, casting laps, warps, inclusions, porosity, ragged edges, surface films such as rolling skin, and other defects which may adversely affect uniform corrosion in service. Anodes shall not be broken.

4. SAMPLING, INSPECTION, AND TEST PROCEDURES

4.1 Unless otherwise specified in the contract or purchase order, the supplier is responsible for the performance of all inspection requirements as specified herein. Except as otherwise specified, the supplier may utilize his own facilities or any commercial laboratory acceptable to the Government. The Government reserves the right to perform any of the inspections set forth in the specification where such inspections are deemed necessary to assure that supplies and services conform to prescribed requirements.

4.2 Lot. Unless otherwise specified in the contract or order (see 6.2), a lot shall consist of all anodes of one shape and type in a single shipment. When practicable, each lot shall be made up of anodes of the same melt, size, and weight.

4.3 Sampling. Unless otherwise specified and when applicable, sampling plans and procedures in the determination of the acceptability of products submitted by a supplier shall be in accordance with the provisions set forth in MIL-STD-105.

4.3.1 *Lot acceptance samples.*

4.3.1.1 *For visual examination.* Sample anodes for visual examination shall be selected from each lot of anodes in accordance with the provisions of MIL-STD-105.

4.3.1.2 *For chemical analysis and microscopic examination.* Sample anodes shall be selected as follows:

(a) For ball anodes or sheared bar and shapes not exceeding 4 inches in length, 4 sample anodes shall be selected at random from each lot.

(b) For shapes other than balls or sheared bar and shapes not exceeding 4 inches in length, at least 2 sample anodes shall be selected at random from each lot, or from each melt if the lot consists of more than one melt. If the melt or melts cannot be identified, at least 4 anodes shall be selected at random from each lot.

4.3.1.2.1 *For chemical analysis.* A composite sample of at least 2 ounces of chips or drillings obtained by drilling or machining the sample anodes of 4.3.1.2, in accordance with method 111 of Fed. Test Method Std. No. 151. Chips or drillings shall be cleaned with a magnet. The sample shall be free from dirt, oil, grit, and other foreign matter. Anodes which have been drilled or machined for chemical analysis may be included in the lot for shipment.

4.3.1.2.2 *For spectrochemical analysis.* Two rod electrodes shall be prepared from each of two anodes in accordance with method 112 of Fed. Test Method Std. No. 151. The samples shall be prepared by conventional methods, suitable for correct applications and usages of the techniques employed. The samples shall be free from dirt, oil, grit, and other foreign matter. Anodes, except for ball type, from which electrodes have been obtained may be included in the lot for shipment.

4.3.1.2.3 *For microscopic examination.* Type II and type III anodes that have been drilled or machined for chemical analysis under 4.3.1.2.1 and 4.3.1.2.2 shall be employed for the determination of the presence of cuprous oxide.

4.4 Lot acceptance examination.

4.4.1 *Anodes.* Sample anodes selected in accordance with 4.3.1.1 shall be visually examined for conformance to the requirements of 3.2, 3.5 and 3.6. Acceptance criteria shall be in accordance with MIL-STD-105 inspection level II, acceptable quality level 1.5 percent.

4.4.2 *Packing and marking.* Packing and marking of the anodes shall conform to this specification.

4.5 Lot acceptance tests.

4.5.1 *Chemical composition.* Sample anodes selected in accordance with 4.3.1.2 shall be tested in accordance with method 111 or 112 of Fed. Test Method Std. No. 151 to determine conformance to the chemical requirements of table I. If the sample fails to conform to the requirements of table I, the lot shall be rejected.

4.5.2 *Cuprous oxide.* Sample anodes selected in accordance with 4.3.1.2.3 shall be tested for the presence of cuprous oxide

The oxide shall be determined by microscopic examination at 75 diameters magnification for compliance with 3.4. Any sample found to contain cuprous oxide shall reject the lot.

5. PREPARATION FOR DELIVERY

(For civil agency procurement, Fed. Std. No. 102 should be referred to for the definitions and applications of the levels of preservation, packaging and packing protection.)

5.1 **Packing.** When practicable, anodes of the same size shall be packed together. Unless otherwise specified, the gross weight of each box shall not exceed approximately 200 pounds.

5.1.1 *Level A*. Anodes shall be packed in boxes in accordance with PPP-B-601 (overseas type), or PPP-B-621 (overseas type).

5.1.2 *Level B*. Anodes shall be packed in domestic type boxes in accordance with PPP-B-585, PPP-B-601, or PPP-B-621.

5.1.3 *Level C*. Anodes shall be packed or otherwise prepared for shipment to insure carrier acceptance and to insure safe delivery to destination at the lowest applicable rate. Containers shall meet, as a minimum, the requirement of rules and regulations applicable to the mode of transportation selected.

5.2 **Marking.**

5.2.1 *Civil agencies*. In addition to any special marking required by the contract or order (see 6.2), shipping containers shall be marked in accordance with Fed. Std. No. 123.

5.2.2 *Military agencies*. In addition to any special marking required by the contract or order (see 6.2), shipping containers shall be marked in accordance with MIL-STD-129.

5.2.3 *Specific markings*. Each container shall be marked with the following:

(a) Specification number
(b) Type and nomenclature, as applicable
(c) Contractor
(d) Contract number or order number
(e) Quantity
(f) Gross weight

6. NOTES

6.1 **Intended use.** Copper anodes are intended for use in copper-plating baths.

6.1.1 *Performance*. Cast, forged, rolled, or electrolytic copper anodes are satisfactory in cyanide copper baths. Cast and rolled anodes are satisfactory in acid copper baths but there is some evidence that electrolytic copper anodes are less satisfactory in this type of bath. There is also some evidence that oxygen free anodes produce less sludge in cyanide baths and that oxygen free, phosphorus bearing anodes are more satisfactory in this respect in acid copper baths.

6.2 **Ordering data.** Purchasers should exercise any desired options offered herein and procurement documents should provide the following (see 4.1 and 4.3):

(*a*) Title, number, and date of this specification.
(*b*) Size, shape and method of suspension (when applicable) (3.2).
(*c*) Composition, if different from 3.3.
(*d*) Size of lot, if different from 4.2.
(*e*) Whether level A, level B, or level C packing is required (5.1.1, 5.1.2, and 5.1.3).
(*f*) Additional marking, if necessary (5.2).
(*g*) Bid sample, if necessary (6.4).

6.3 **Methods of chemical analysis.** It is intended that the chemical analysis be conducted so that no particular method of analysis be specified. As a guide, copper content in anodes may be determined in accordance with ASTM Designation E-53, Method for Chemical Analysis of Copper (Electrolytic Determination of Copper). Metallic impurities in copper anodes may be determined by spectrographic methods in accordance with ASTM Designation E-2 SM5-2, Spectrochemical Analysis of Wrought Copper Alloy by the DC Arc Technique or photometric methods in accordance with ASTM Designation E62, Standard Photometric Methods for Chemical Analysis of Copper or Copper-Based Alloys.

6.4 It is believed that this specification adequately describes the characteristics necessary to secure the desired material, and that normally no samples will be necessary prior to award to determine compliance with this specification. If, for any particular purpose, samples with bids are necessary, they should be specifically asked for in the invitation for bids, and the particular purpose to be served by the bid sample should be definitely stated, the specification to apply in all other respects.

6.5 **Transportation Description.** Transportation descriptions and minimum weights applicable to this commodity are:

Rail:

Anodes, copper.
Carload minimum weight 40,000 pounds

Motor:

Anodes, copper.
Truckload minimum weight 40,000 pounds, subject to Rule 115, National Motor Freight Classification.

Notice. When Government drawings, specifications, or other data are used for any purpose other than in connection with a definitely related Government procurement operation, the United States Government thereby incurs no responsibility nor any obligation whatsoever; and the fact that the Government may have formulated, furnished, or in any way supplied the said drawings, specifications, or other data, is not to be regarded by implication or otherwise as in any manner licensing the holder or any other person or corporation, or conveying any rights or permission to manufacture, use, or sell any patented invention that may in any way be related thereto.

MILITARY CUSTODIANS:

Army—WC

Navy—Wep

Air Force—WRAMA (Code 84)

U S GOVERNMENT PRINTING OFFICE: 1964—O-739-664/264

Copies of this specification may be purchased for 5 cents each.

DISTRIBUTION LIST FOR MARTIN MARIETTA
FINAL REPORT ON CONTRACT DAAG46-74-C-0128

Commander U.S. Army Materiel Development and Readiness Command ATTN: DRCLDC, Dr. R. Zentner 5001 Eisenhower Avenue Alexandria, VA 22333	 1
Ballistic Missile Defense Program Office ATTN: DACS-BMT, Mr. C. McClain DACS-BMT, Mr. V. Kupelian Commonwealth Bldg., Room 1100 1300 Wilson Blvd. Arlington, VA 22209	 1 1
Director Ballistic Missile Defense Advanced Technology Center ATTN: ATC-M, Dr. D. Harmon ATC-M, Mr. M. Whitfield ATC-S, Mr. W. Loomis P. O. Box 1500 Huntsville, AL 35807	 1 1 1
Commander Ballistic Missile Defense Systems Command ATTN: SSC-TEN, Mr. N. J. Hurst P. O. Box 1500 Huntsville, AL 35807	 1
Director Defense Nuclear Agency ATTN: SPAS, Mr. J. F. Moulton, Jr. SPAS, Mr. M. Rubenstein Washington, D. C. 20305	 1 1
Office of Secretary of Defense Office of the Director of Defense Research and Engineering ATTN: Mr. J. Persh, Staff Specialist for Materials and Structures The Pentagon Washington, D. C. 20301	 1

Office of Chief, Research Development and Acquisition
Department of the Army
ATTN: DAMA-CSS, Dr. J. Bryant 1
Washington, D. C. 20310

Commander
Harry Diamond Laboratories
ATTN: AMXDO-RC, Dr. R. Oswald 1
AMXDO-NP, Dr. F. Wimenitz 1
AMXDO-NP, Mr. J. Gwaltney 1
AMXDO-NP, Mr. J. J. Corrigan 1
2800 Powder Mill Road
Adelphi, MD 20783

Commander
Picatinny Arsenal
ATTN: Mr. M. Allen 1
Mr. M. Weinstein 1
Mr. B. Frank 1
Dover, NJ 07801

Commander
U. S. Army Combat Development Command
ATTN: Technical Library 1
Institute of Nuclear Studies
Fort Bliss, Texas 79916

Commander
Air Force Materials Laboratory
Air Force Systems Command
ATTN: MXS/Maj. H. Keck 1
MBC/Dr. D. Schmidt 1
LNE/Mr. G. Schmitt 1
Wright-Patterson Air Force Base, Ohio 45433

Effects Technology, Inc.
ATTN: Mr. J. Green 1
P. O. Box 30400
Santa Barbara, CA 93105

General Electric Company
Valley Forge Space Technology Center
ATTN: Mr. K. Hall 1
Mr. J. Brazel 1
P. O. Box 8555
Philadelphia, PA 19101

Kaman Sciences Corporation	
ATTN: Mr. F. Shelton	1
P. O. Box 7463	
Colorado Springs, CO 80933	
Ktech	
ATTN: Dr. D. Keller	1
911 Pennsylvania Avenue, N.E.	
Albuquerque, NM 87110	
Lockheed Missiles and Space Company	
ATTN: Mr. D. Aspinwall	1
P. O. Box 504	
Sunnyvale, CA 94088	
Martin Marietta Corporation	
ATTN: Mr. R. Dowd	1
Mr. L. Kinnaird	1
Mr. A. Ossin	1
Mr. P. Kendall	1
Mr. J. Potts	1
Mr. W. Bauman	1
Mr. R. Howell	1
P. O. Box 5837	
Orlando, Florida 32805	
McDonnell Douglas Corporation	
ATTN: Mr. H. Hurwicz	1
Mr. G. Roark	1
Mr. J. Wuehrer	1
5301 Bolsa Avenue	
Huntington Beach, CA 92647	
Commander	
Naval Ordnance Systems Command	
ATTN: ORD-02331, Mr. M. Kinna	1
Washington, D. C. 20360	
Commander	
Naval Surface Weapons Center	
ATTN: Mr. D. Goldstein	1
Mr. C. Rowe	1
Mr. C. Lyons	1
Mr. F. Koubek	1
Silver Springs, MD 20910	

Los Alamos Scientific Laboratory
ATTN: GMX-6, Dr. J. W. Taylor 1
P. O. Box 1663
Los Alamos, NM 87544

Space and Missile Systems Organization
ATTN: RSSE/Maj. J. McCormack 1
RSSE/Lt. S. Kreighbaum 1
RSSE/Capt. D. Jackson 1
P. O. Box 92960
World Way Postal Center
Los Angeles, CA 90009

Sandia Laboratories
ATTN: Mr. J. K. Cole 1
P. O. Box 5800
Albuquerque, NM 87115

Aerospace Corporation
ATTN: Dr. L. Rubin 1
Mr. J. D. McClelland 1
Dr. R. Halise 1
P. O. Box 92957
Los Angeles, CA 90009

Aeronautical Research Associates of Princeton
ATTN: Dr. C. Donaldson 1
50 Washington Road
Princeton, NJ 08540

AVCO Systems Division
ATTN: Mr. D. Rolincik 1
Mr. V. DiCristina 1
201 Lowell Street
Wilmington, MA 01887

Battelle Memorial Institute
ATTN: Mr. Hugh Hanes 1
505 King Avenue
Columbus, Ohio 43201

Institute for Defense Analysis
ATTN: Mr. Ellis L. Foster, Jr. 1
400 Army-Navy Drive
Arlington, VA 22202

Prototype Development Associates	
ATTN: Dr. J. I. Slaughter	1
Dr. J. McDonald	1
Dr. S. S. Dunn	1
1740 Garry Avenue, Suite 201	
Santa Ana, CA 92705	
R & D Associates	
ATTN: Dr. A. Field	1
P. O. Box 9695	
Marina del Rey, CA 92664	
Southwest Research Institute	
ATTN: Mr. A. Wenzel	1
8500 Culebra Road	
San Antonio, Texas 78206	
Stanford Research Institute	
ATTN: Dr. G. Abrahamson	1
333 Ravenswood Avenue	
Menlo Park, CA 90250	
Terra Tek, Inc.	
ATTN: Dr. A. H. Jones	1
University Research Park	
420 Wakara Way	
Salt Lake City, Utah 84108	
TRW Systems Group	
ATTN: Mr. D. Gamble	1
Mr. D. Bauer	1
Mr. I. Rubin	1
One Space Park	
Redondo Beach, CA 90278	
Defense Documentation Center	2
Cameron Station, Bldg. 5	
5010 Duke Street	
Alexandria, VA 22314	

Director
Army Materials and Mechanics Research Center

ATTN:	DRXMR-H, Mr. J. F. Dignam	1
	DRXMR-H, Mr. L. R. Aronin	1
	DRXMR-H, Dr. S. C. Chou	1
	DRXMR-H, Maj. L. Abramson	1
	DRXMR-AP	1
	DRXMR-PL	2
	DRXMR-PR	1

Watertown, MA 02172

Army Materials and Mechanics Research Center,
Watertown, Massachusetts 02172
EVALUATION OF CONAP CONCEPT FOR ADVANCED ABM NOSETIPS
Archie Ossin and Paul Kendall
Martin Marietta, Aerospace
Orlando, Florida 32805
Technical Report AMMRC CTR 76-38, November 1976,
104 pp-illus-tables, Contract DAAG46-74-C-0128
D/A Project 1W162113A661,
AMCMS Code 62113.11.07000,
Final Report, 29 May 1974 to 30 June 1976

AD ______

UNCLASSIFIED
UNLIMITED DISTRIBUTION

Key Words

Missiles
Anti-missile missiles
Nose cones
Cooling systems
Transpiration
Gas permeability
Porous metals

Unclassified Report

This document reports the results of a 25-month research study, entitled "Evaluation of CONAP concept for Advanced ABM Nosetips." This program evaluated the performance of the Controlled Atmosphere Protection (CONAP) concept in active oxidation protection of a hot refractory metal, transpiration cooled nosetip for future application in an Advanced Interceptor Missile system. The specific objectives of this program were to build, process, test, and evaluate three-dimensional porous tungsten, sphere-cone nosetips at the Wright-Patterson 50 MW Plasma Arc Facility. In addition, the program evaluated distributed discrete hole models in the Martin Marietta Ramburner Facility. The porous tungsten nosetips, tested in the 50 MW Plasma Arc Facility were processed porous tungsten made from Sylvania Tungsten-Copper (80 v/o W - 20 v/o Cu), manufactured to SPRINT Specification 11181124. This material selection was based on the results of previous work accomplished under AMMRC Contract DAAG46-73-C-0053 where several porous tungsten materials were characterized for flow properties and internal heat transfer characteristics. The results of these tests showed that the CONAP Concept was viable; however, further development of the porous tungsten material will be required for use in a flight environment. A significant result of the evaluation of the discrete hole concepts was that a departure from the ordinary sphere-cone configuration was advantageous in terms of requiring a minimum flow for survival.

Army Materials and Mechanics Research Center,
Watertown, Massachusetts 02172
EVALUATION OF CONAP CONCEPT FOR ADVANCED ABM NOSETIPS
Archie Ossin and Paul Kendall
Martin Marietta, Aerospace
Orlando, Florida 32805
Technical Report AMMRC CTR 76-38, November 1976,
104 pp-illus-tables, Contract DAAG46-74-C-0128
D/A Project 1W162113A661,
AMCMS Code 62113.11.07000,
Final Report, 29 May 1974 to 30 June 1976

AD ______

UNCLASSIFIED
UNLIMITED DISTRIBUTION

Key Words

Missiles
Anti-missile missiles
Nose cones
Cooling systems
Transpiration
Gas permeability
Porous metals

Unclassified Report

This document reports the results of a 25-month research study, entitled "Evaluation of CONAP concept for Advanced ABM Nosetips." This program evaluated the performance of the Controlled Atmosphere Protection (CONAP) concept in active oxidation protection of a hot refractory metal, transpiration cooled nosetip for future application in an Advanced Interceptor Missile system. The specific objectives of this program were to build, process, test, and evaluate three-dimensional porous tungsten, sphere-cone nosetips at the Wright-Patterson 50 MW Plasma Arc Facility. In addition, the program evaluated distributed discrete hole models in the Martin Marietta Ramburner Facility. The porous tungsten nosetips, tested in the 50 MW Plasma Arc Facility were processed porous tungsten made from Sylvania Tungsten-Copper (80 v/o W - 20 v/o Cu), manufactured to SPRINT Specification 11181124. This material selection was based on the results of previous work accomplished under AMMRC Contract DAAG46-73-C-0053 where several porous tungsten materials were characterized for flow properties and internal heat transfer characteristics. The results of these tests showed that the CONAP Concept was viable; however, further development of the porous tungsten material will be required for use in a flight environment. A significant result of the evaluation of the discrete hole concepts was that a departure from the ordinary sphere-cone configuration was advantageous in terms of requiring a minimum flow for survival.

Army Materials and Mechanics Research Center,
Watertown, Massachusetts 02172
EVALUATION OF CONAP CONCEPT FOR ADVANCED ABM NOSETIPS
Archie Ossin and Paul Kendall
Martin Marietta, Aerospace
Orlando, Florida 32805
Technical Report AMMRC CTR 76-38, November 1976,
104 pp-illus-tables, Contract DAAG46-74-C-0128
D/A Project 1W162113A661,
AMCMS Code 62113.11.07000,
Final Report, 29 May 1974 to 30 June 1976

AD ______

UNCLASSIFIED
UNLIMITED DISTRIBUTION

Key Words

Missiles
Anti-missile missiles
Nose cones
Cooling systems
Transpiration
Gas permeability
Porous metals

Unclassified Report

This document reports the results of a 25-month research study, entitled "Evaluation of CONAP concept for Advanced ABM Nosetips." This program evaluated the performance of the Controlled Atmosphere Protection (CONAP) concept in active oxidation protection of a hot refractory metal, transpiration cooled nosetip for future application in an Advanced Interceptor Missile system. The specific objectives of this program were to build, process, test, and evaluate three-dimensional porous tungsten, sphere-cone nosetips at the Wright-Patterson 50 MW Plasma Arc Facility. In addition, the program evaluated distributed discrete hole models in the Martin Marietta Ramburner Facility. The porous tungsten nosetips, tested in the 50 MW Plasma Arc Facility were processed porous tungsten made from Sylvania Tungsten-Copper (80 v/o W - 20 v/o Cu), manufactured to SPRINT Specification 11181124. This material selection was based on the results of previous work accomplished under AMMRC Contract DAAG46-73-C-0053 where several porous tungsten materials were characterized for flow properties and internal heat transfer characteristics. The results of these tests showed that the CONAP Concept was viable; however, further development of the porous tungsten material will be required for use in a flight environment. A significant result of the evaluation of the discrete hole concepts was that a departure from the ordinary sphere-cone configuration was advantageous in terms of requiring a minimum flow for survival.

Army Materials and Mechanics Research Center,
Watertown, Massachusetts 02172
EVALUATION OF CONAP CONCEPT FOR ADVANCED ABM NOSETIPS
Archie Ossin and Paul Kendall
Martin Marietta, Aerospace
Orlando, Florida 32805
Technical Report AMMRC CTR 76-38, November 1976,
104 pp-illus-tables, Contract DAAG46-74-C-0128
D/A Project 1W162113A661,
AMCMS Code 62113.11.07000,
Final Report, 29 May 1974 to 30 June 1976

AD ______

UNCLASSIFIED
UNLIMITED DISTRIBUTION

Key Words

Missiles
Anti-missile missiles
Nose cones
Cooling systems
Transpiration
Gas permeability
Porous metals

Unclassified Report

This document reports the results of a 25-month research study, entitled "Evaluation of CONAP concept for Advanced ABM Nosetips." This program evaluated the performance of the Controlled Atmosphere Protection (CONAP) concept in active oxidation protection of a hot refractory metal, transpiration cooled nosetip for future application in an Advanced Interceptor Missile system. The specific objectives of this program were to build, process, test, and evaluate three-dimensional porous tungsten, sphere-cone nosetips at the Wright-Patterson 50 MW Plasma Arc Facility. In addition, the program evaluated distributed discrete hole models in the Martin Marietta Ramburner Facility. The porous tungsten nosetips, tested in the 50 MW Plasma Arc Facility were processed porous tungsten made from Sylvania Tungsten-Copper (80 v/o W - 20 v/o Cu), manufactured to SPRINT Specification 11181124. This material selection was based on the results of previous work accomplished under AMMRC Contract DAAG46-73-C-0053 where several porous tungsten materials were characterized for flow properties and internal heat transfer characteristics. The results of these tests showed that the CONAP Concept was viable; however, further development of the porous tungsten material will be required for use in a flight environment. A significant result of the evaluation of the discrete hole concepts was that a departure from the ordinary sphere-cone configuration was advantageous in terms of requiring a minimum flow for survival.